Technische Universität Berlin

Institute für Luft- und Raumfahrt

Fachgebiet Raumfahrttechnik

Fakultät V

Marchstraße 12-14
10587 Berlin

http://www.ilr.tu-berlin.de/menue/home/

Master Thesis

Concept and Simulation of an Antenna Tracking System for Sounding Rockets

Şükrü KILIK

Matriculation Number: 0370826

01.11.2017

Supervised by:

Prof. Dr. Klaus Brieß

Assistant Supervisor

Sebastian Trowitzsch

Acknowledgements

First of all, I would like to thank Prof. Klaus Brieß at the Chair of Space Technology for giving me the opportunity to carry out state of the art research in this field.

Special thanks to Mister Sebastian Trowitzsch for his guidance and friendly behaviour. Moreover, also special thanks to Mister Cem Avsar and Miss Olga Homakova for help and guidance during my study in MSE – It would be not possible to finish the study without them.

Furthermore, I would like to thank Ministry of National Education of Turkey to finance my study in TU Berlin.

Last but not least, special thanks to Miss Svoboda Kunina for her encouragement and support.

Declaration of Authorship

I hereby certify that this thesis has been composed by me and is based on my own work unless stated otherwise. No other person's work has been used without due acknowledgement in this thesis. All references and verbatim extracts have been quoted, and all sources of information, including graphs and data sets, have been specifically acknowledged.

Place and date

Signature

Agreement on rights of utilization

The Technische Universität Berlin, represented by the Chair of Space Technology, may use the results of the thesis at hand in education and research. It receives simple (non-exclusive) rights of utilization as according to § 31 Abs. 2 Urheberrechtsgesetzt (Urhg). This right of utilisation is unlimited and involves content of any kind (e.g. documentation, presentations, animations, photos, videos, equipment, parts, procedures, designs, drawings, software including source code and similar). An eventual commercial use on part of the Technische Universität Berlin will only be carried out with approval of the author of the thesis at hand under appropriate share of earnings.

Place and date

Signature

Professor Dr.-Ing. Klaus Brieß

Head of the Chair of Space Technology

Abstract

One of the key studies in atmospheric science is examining and understanding the effects of human-made greenhouse gases in the atmosphere. “Indonesian National Institute for Aeronautics and Space” and “Chair of Space Technology in TU Berlin” established a mission, which is called as “Development Support for RX-320 sounding rocket payload compartment and atmospheric payload”, to do measurements, in the stratosphere and troposphere layers, such as temperature, pressure, humidity, wind speed and direction, Ozone and CO2 densities. According to operational requirements of the mission, the payload shall be launched by the RX-320 sounding rocket up to 40 km altitude and be separated by the separation system which is developed by TU Berlin and descent with a parachute with a defined average rate to the ground.

On the telecommunication point of view, channel capacity can increase remarkably by employing a highly directive antenna for receiving telemetry signal. Due to, the beamwidth of directional antennas are narrow; an antenna tracking concept must be realised to support the reception of the payload data during launch and descent phases. This thesis focuses on designing antenna tracking system for sounding rockets with the example of RX-320. This thesis presents how to find the direction of arrival of the telemetry signal from the rocket and track the signal to achieve antenna tracking duty.

In this thesis, MATLAB and Simulink simulation tools are used to determine optimum tracking system parameters. FH/BPSK spread spectrum signals are considered as telemetry signal. The noise in the channel is assumed as independent additive white Gaussian noise. The Doppler frequency shift in the signal due to the sounding rocket movement is much smaller than signal bandwidth. The simulation shows that cross-correlation tracking method is appropriate to track sounding rockets which have FH/BPSK as a telemetry signal.

Table of Contents

List of Figures

1 Introduction

1.1 Problem Description

One of the critical studies in atmospheric science is examining and understanding the effects of human-made greenhouse gases in the atmosphere. “Indonesian National Institute for Aeronautics and Space” and “Chair of Space Technology in TU Berlin” established a mission, which is called as “Development Support for RX-320 sounding rocket payload compartment and atmospheric payload”,to do measurements, in the stratosphere layer, such as temperature, pressure, humidity, wind speed and direction, Ozone and CO2 densities. According to operational requirements of the mission, the payload shall be launched by the RX-320 sounding rocket up to 40 km altitude and be separated by the separation system which is developed by TU Berlin and descent with a parachute with a defined average rate to the ground.

On the ground segment of the mission, an antenna tracking concept must be realised to support the reception of the payload data during launch and descent phases. All the telemetry shall be received by more than one ground stations along the launcher and payload descending trajectory for redundancy. Receiving telemetry and tracking the signals can be done by observing stations [1].

There are some difficulties in tracking moving target manually. One of the most critical ones is a fading on telemetry signal with the reason of large error angle between the direction of communication antenna and payload. The accuracy of tracking depends on the ability of the operator in manual tracking systems. Especially, tracking fast-moving targets in long distances can be beyond of human predictions.

Furthermore, on the communication point of view, work has been done by G. Chen et al. [2], Sultan Aljahdali [3], and Tiago Varum et al. [4] that shows how the system capacity can increase remarkably by employing a highly directive antenna along with a tracking system. Opposingly, how the system capacity can be penalised by increasing antenna pointing error. An advancement in link budget, and therefore channel capacity, will also allow for better link margin on the receiver site (ground station).

The source of motivation for this research is the need of realising uninterrupted telemetry between payload and ground station. According to the mission scenario of the RX-320 Atmospheric Payload three different automatic tracking concepts are considered for concurrent implementation to track the payload;

1. Using tracking information delivered by the primary ground station at LAPAN`s rocket technology centre, the respective elevation and azimuth angles are

calculated for the second ground station which is located 1.5 km away from the primary ground station.

2. The GPS data of the payload`s GPS receiver is excerpted from the data stream and used for pointing the second ground station antennas whose exact position is also well known.
3. Directional information is delivered by the reception of the payload data itself to point the antenna towards the payload. This information can be retrieved by analysing the signal using multiple antennas.

This dissertation will focus on the third strategy for antenna pointing and track the payload.

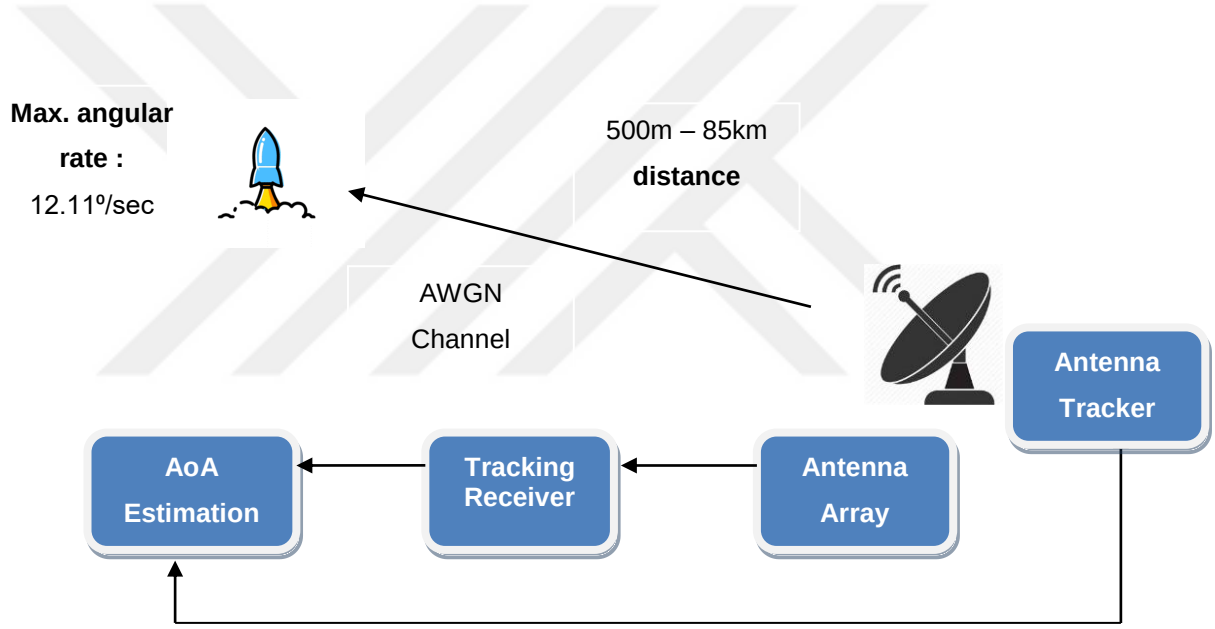

Figure 1.1: Automatic Antenna Tracking System

The automatic antenna tracking system consists of 5 sections which are Target (payload), an Antenna array, Receiver, Angle of Arrival Estimation, and Antenna Tracker.

1.2 Specification of the Target

There are two different phases of the mission. The first is the launch phase and the second is descending phase. According to flight report, Indonesian colleagues provide, the maximum angular rate of the target with respect to the tracking antenna array is 12.11º/sec. and the distance changes from 500 m to 85 km. The target has been tracked by telemetry signal. The level of signal power is estimated around -90 dBm. Therefore, the sensitivity of tracking receiver should be -97dBm. The communication channel assumed Additive White Gaussian Noise (AWGN).

It is assumed that the target payload has BPSK modulation shame and using Frequency Hopping Spread Spectrum Technique for spreading the signal. Because of the frequency allocations regulation and availability issues, payload transmitter is using 2.4GHz-to-2.4835 GHz ISM band.

The communication antenna dish has 6ºs of Full Wave Half Maximum (FWHM) beam width. Therefore, the requirement for maximum error angle should be 3ºs. The frequency is hopping around 27 MHz. To achieve the tracking frequency hopping spread spectrum signal without the hopping knowledge, the tracker should observe the whole frequency spectrum which the signal is hoping. For these reasons an algorithm for tracking telemetry signal should detect and estimate the angle of arrival of the wideband telemetry signal.

1.3 Estimation of Direction of Arrival

There are two crucial steps to tracking the sounding rocket. The first step is scanning the target in RADAR range. It is assumed that direction of the rocket is known before the mission begins. Issues like scanning switching noise and squint angle are avoided by this way. Therefore, the first and the most critical goal of tracking the sounding rocket is determining the angle of arrival (DOA) of telemetry signal.

Phase interferometer technique is proposed to estimate DOA as an appropriate method which meets the requirements of the sounding rocket tracking system. Cross-Correlation of the signals on antenna elements is calculated to extract phase difference information between antennas. However, for high frequencies (Because the wavelength is short) phase ambiguity becomes a major problem. Unambiguous estimation of AoA requires ambiguity solving algorithm and 3 or more antennas for every dimension of the array. Figure 1.2 shows a functional block diagram of DOA estimator.

1.4 Antenna Array and

According to the mission requirements, telemetry signal will be in 2.4GHz-to-2.4835 GHz ISM band. Therefore, the risk of getting interference signal is high. For the sake of solve interference problem using highly directional antennas in tracking receiver is necessary. On the other hand, applying highly directional antenna makes challenging to track the rocket and payload. The tracking receiver system should respond fast thus the DOA estimation algorithm should be computationally light.

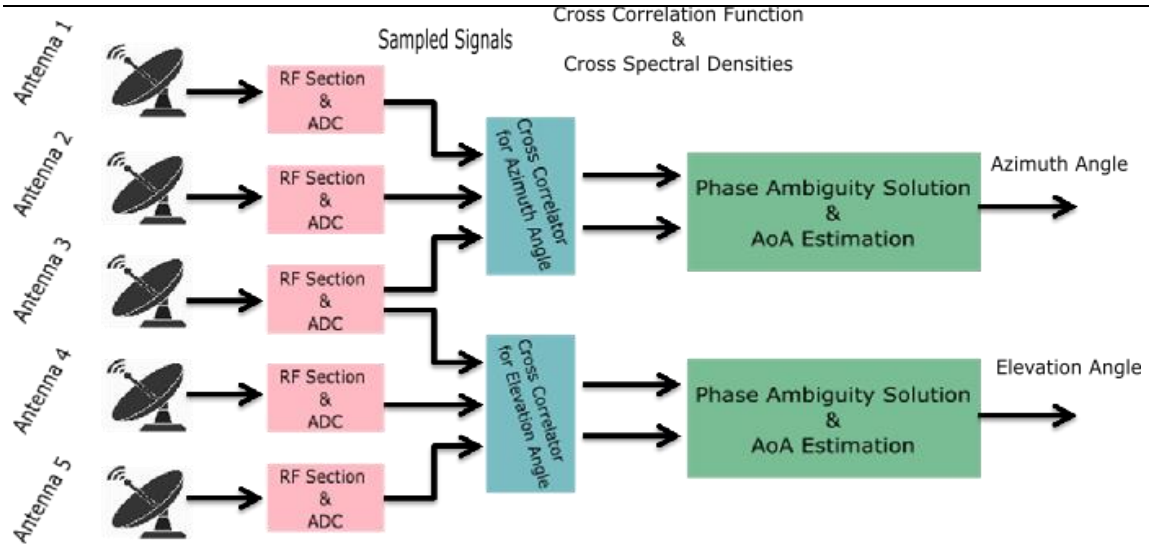

Figure 1.2: Functional Block Diagram of AoA Estimation

The Frequency of the telemetry signal and the DOA estimation algorithm defines the geometry of the antenna array and the tracking receiver.

The most basic case for antenna tracking is estimating AoA of the telemetry signal and tracking the target in 1-Dimensional space without phase ambiguity. AoA estimation is realised by measuring the phase difference between the signals which received by two antennas. However, this approach is only valid when the two receiver antennas in the smaller distance than half of the wavelength (λ=c/f) of telemetry signal.

However, in the case of the distance between antennas is bigger than half of the wavelength, phase ambiguity problem occurs due to the periodic nature of the telemetry signal. Algorithms created to solve the ambiguity problem uses the third antenna for every dimension.

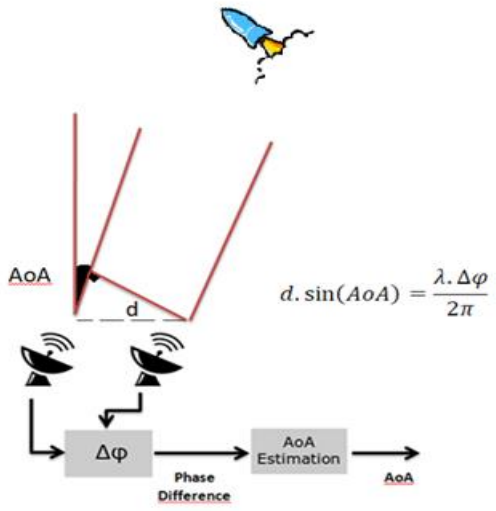

Figure 1.3: Two Antennas One Dimensional Tracking

To track the target in 2-Dimensions (azimuth and elevation) we need planar antenna array instead of linear. When there is no phase ambiguity, four antennas are enough to track the target in 2-D space. However, due to the high frequency (short wavelength) we work, a solution should be found for phase ambiguity problem.

Adding one more antenna for every dimension is required to solve the problem. However, this problem has been solved by only using one extra antenna by using a common antenna in azimuth and elevation dimensions.

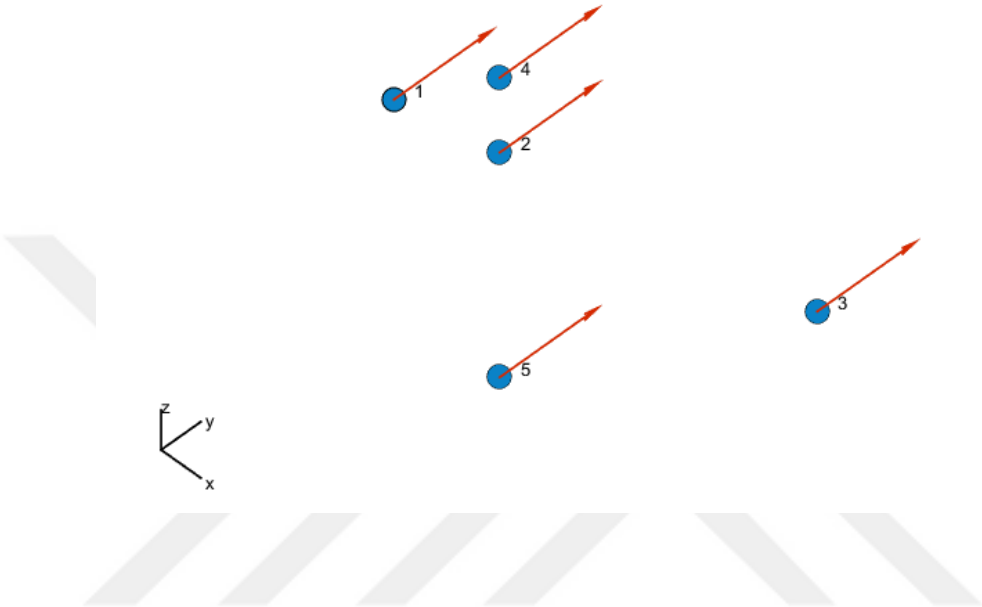

Figure 1.4: 2-D Antenna Array Configurations for Tracking Receiver

1.5 Scope of thesis

This dissertation includes seven chapters. In the second chapter different spread spectrum communication techniques has been described and especially the frequency hopping spread spectrum technique, which is the spreading method for our system, explained. Antenna Arrays has been described in chapter three, in this chapter basic antenna parameters, fundamentals of antenna arrays and smart antennas described in detail. The antenna array which has designed for tracking system also described in this chapter. The literature review for the direction of arrival estimating systems has been written in chapter four in detail. In that chapter, the answer to the question of “Why the cross-correlation Interferometry technique has been used for tracking sounding rockets?” is given. Cross-correlation interferometry method has been described in detail in chapter five. Simulation methodology the project is described, and the results of computer simulation argued in chapter six. Finally, the proposed system has been explained in chapter seven.

2 Spread Spectrum Communication Techniques

According to mission scenario of Antenna Tracking Concept, the telemetry signal of the payload of the sounding rocket is in the scheme of Frequency Hopping Spread Spectrum signal. Therefore, firstly spread spectrum communication technique will be introduced, and frequency hopping spread spectrum technique will be explained in this chapter.

In the case of using ISM bands, the possibility of an encounter with interference is high. Hence, the telemetry signal should be sent to a technique which ensures secured communication. Spread spectrum communication techniques are wideband communication techniques which protect the telemetry signal from jamming and decrease the possibility of being detected by unauthorised receivers. There are many spread spectrum techniques. For the sake of not drift away from the main topic, Direct Sequence Spread Spectrum method will only be mentioned, and Frequency Hopping Spread Spectrum Method will be explained more.

2.1 Direct Sequence Spread Spectrum Method

The most fundamental spread spectrum communication technique is Direct Sequence Spread Spectrum(DS/SS). According to this technique, the transmitter of the payload multiplies data signal (m(t)) with Pseudo Noise (PN) code signal (c(t)). This multiplication process spreads the data signal to wideband and makes the output signal power level in a level of noise which in transmitting media.

The bandwidth of the data signal spread by N which is the length of the PN code. Therefore, N is also called as a Spreading Factor. With this technique, the transmitter generates a different PN code for every authorised receiver and receivers know the PN code has generated for themselves.

For a receiver part, every receiver multiplies the received signal by PN code, which is dedicated to that receiver, to interpret the data signal back. Figure 2.1 shows the principle of Direct Sequence Spread Spectrum Communication System.

Usually, some of the spread spectrum techniques, like CDMA, are designed as a multiplexing method to use in mobile communication. Moreover, the number of receivers can be supported, determined by the length of PN code (N). Therefore, there are many ways to generate more extended PN code sequence. The most important ones are Maximum Length PN sequences, Gold Sequences, Kasami Sequences and Walsh Hadamart Sequences. Whichever method has been chosen to generate the sequence, PN codes should have some properties like high autocorrelation, low cross-correlation, equal probability of states (1s and -1s).

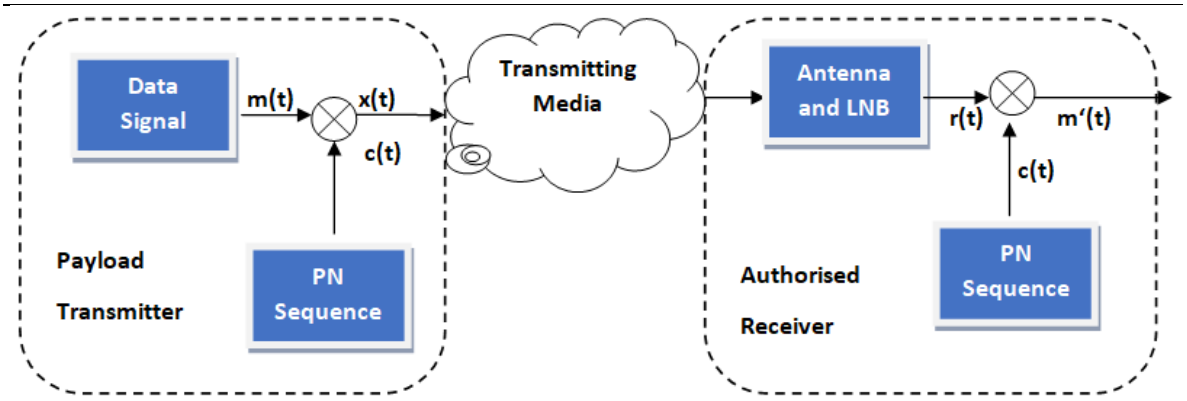

Figure 2.1: Direct Sequence Spread Spectrum Communication System

However, the main reason to use spread spectrum technique in our payload is a high possibility of the interference in ISM bands. In the direct sequence spread spectrum technique, the power of each interferer is suppressed by a factor N which is the length of PN code sequence.

2.2 Frequency Hopping Spread Spectrum Method

In Frequency Hopping Spread Spectrum Technique (FHSS), the entire frequency spectrum divided into smaller channels. In FHSS, the transmitter hops between available narrowband frequencies within specified broad channels in a pseudo-random (PN) sequence known to both sender and receiver. A short burst of data is transmitted on the current narrowband channel, After that, transmitter and receiver tune to the next frequency in the sequence for the next burst of data. On most systems, the transmitter will hop to a new frequency more than twice per second. Because no channel is used for long, and the odds of any other transmitter being on the same channel at the same time are low.

The frequency of the carrier is periodically modified following a specified sequence of frequency. This sequence is known as hopping sequence or spreading code. The amount of time spent on each frequency or hop is known as dwell time or hopping time. Following frequency hopping sequence, the data is modulated by any narrowband modulation technique. At the time of transmission sender first, modulate their signal by using first time-slots' frequency. Once, dwell time is completed then it modulates their signal by using the second time slots' frequency. After third and forth. To receive the data correctly, the receiver should know frequency hopping pattern.

There are two types of frequency hopping: slow frequency hopping spread spectrum and fast frequency hopping spread spectrum. In slow frequency hopping, one or more bits are transmitted within one hop. On the other hand, in the fast frequency hopping one bit is divided over multiple hops. In the slow frequency hopping, coherent data detection is

possible. However, coherent signal detection is difficult, and seldom used in fast frequency hopping. While error control can be done in slow frequency hopping, this is not possible in the fast frequency hopping method.

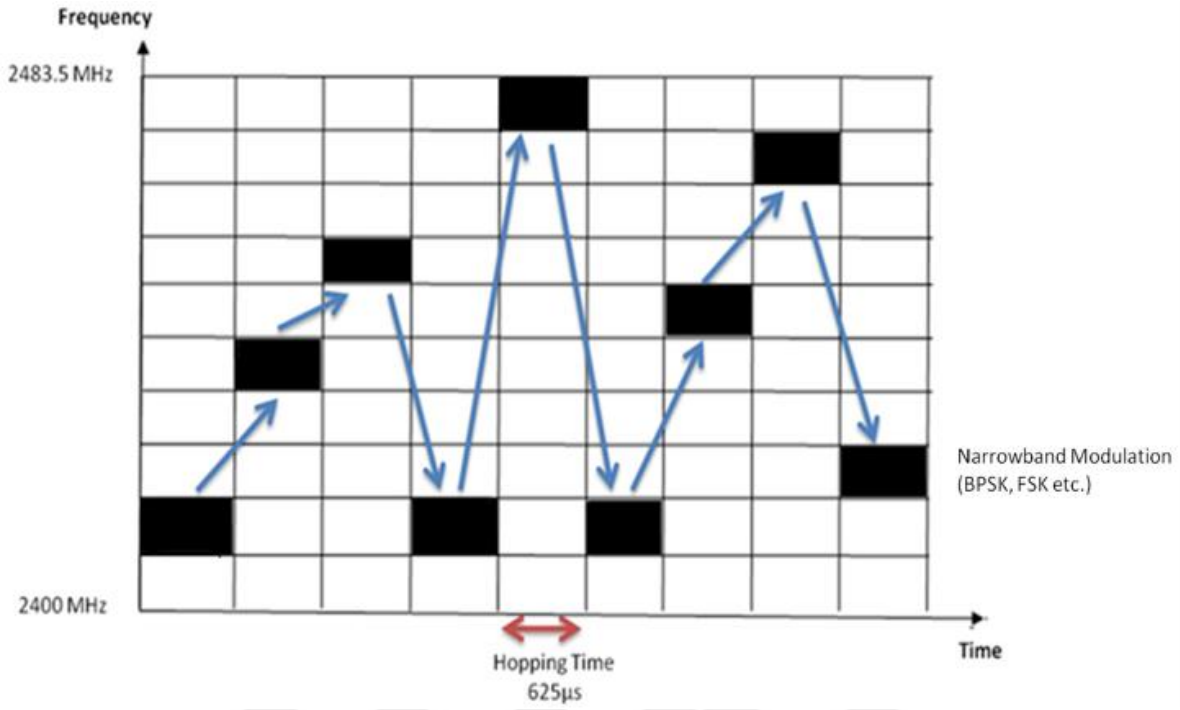

Figure 2.2: Frequency Hopping Pattern for sample FHSS system

2.3 Comparison of Direct Sequence Spread Spectrum and Frequency Hopping Spread Spectrum

This part of dissertation analyses the differences between DSSS and FHSS to understand better the nature of telemetry signal which automatic antenna tracker should track.

According to Federal Communication Commissions' (FCC) rules a communication system need to guarantee to avoid interrupting other radio users. One of the way doing this is reducing the average power spectral density of telemetry signal. It becomes crucial primarily for space applications which use ISM bads. Both FHSS and DSSS reduce the spectral density lower than the noise floor. [11]

Chronologically, first applications of spread spectrum communication are military based due to secure the radio channel from unauthorised receivers. Therefore, interference susceptibility is another critical parameter. DSSS achieve this goal by multiplying the data by PN code sequence. This operation spread the data to all part of the spectrum so having narrowband interference is not a problem. However, DSSS communication system should be well away from high power broadcast stations. FHSS does not stay on one frequency for a long time. However, it sends all the data via the narrowband channel during dwell time. For that reason, if it hits the frequency, which has much interference,

the telemetry signal is lost. Therefore, in a packet switched communication systems re-transmission will occur via the clearer channel. This nature of FHSS leads to bursty nature of errors due to frequency selective fading mainly. Hence DSSS system prone to errors but at low level compare to FHSS systems. FHSS produces strong bursty errors. [1]

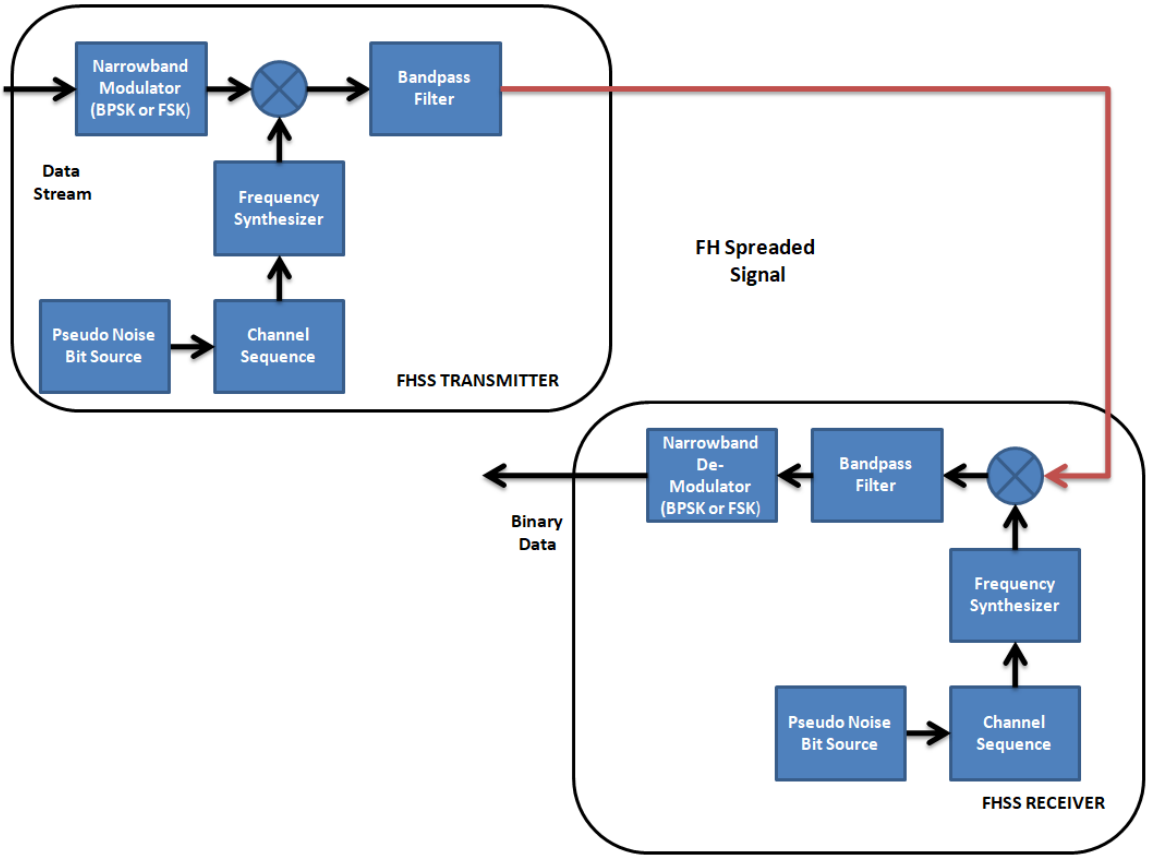

Figure 2.3: Block Diagram of the Frequency Hopping Spread Spectrum System

DSSS can support data rate until 11 Mbps while FHSS can support 3 Mbps. Even though DSSS is more advantageous than FHSS due to this merit, FHSS is very robust technology. This merit is useful in a harsh environment comprising large coverage, multi-path, collocated cells, noises and existence of Bluetooth frequency waves. [1]

Comparing the merits of FH or DS spread spectrum methods is not easy. The choices depend on the particular implementation scenario. In most cases, space applications contain harsh communication media. Furthermore, 2.4 GHz ISM band include many interferences. The fast-moving nature of the payload also adds many fading parameters (like Doppler shift) to the telemetry system. Even though both spreading techniques are available for communicating with the ground station, FHSS has been chosen as a spreading method for this mission.[1]

3 Antenna Arrays

One of the most critical parameters in communication systems is channel capacity. Antenna Arrays and Smart antennas seem like satisfactory concepts for the requirements of the contemporary communication systems. According to operational requirements of the mission, the payload shall be launched by the RX-320 sounding rocket up to 40 km altitude and descent with a parachute with a defined average rate to the ground. Automatic Antenna Tracking System should track the rocket in ascent and the payload in descent phase of the operation to require channel capacity between ground station and payload.

Therefore, basic antenna parameters and fundamentals of antenna array will be described in this chapter. The thing makes antenna arrays smart is signal processing behind. Smart antennas will also be described in this chapter.

3.1 Basic Antenna Parameters

The definition of antenna parameters is essential to define the performance of an antenna array. It will be suitable to mention basic parameters of antenna systems before introducing the antenna arrays.

3.1.1 Radiation Pattern

A graphical presentation of the distribution of the power which is radiated by an antenna as a function of direction angle defined as a radiation pattern of that antenna [12]. The radiation pattern can be determined in the far field region of the antenna and is represented as a function of the directional coordinates.

We can separate the space surrounding the antenna by three regions as reactive near field, near field (Fresnel) and far-field (Fraunhofer) [12]. Although there is no sudden change in the transitions of these areas, there are significant differences between them.

Reactive near field; is an area which reactive area is predominant and is defined as the immediate area surrounding the near-field area. The energy storage is observed in this area instead of spreading, and the reactive near-field region is defined as equation 3.1 for most antennas:

$$R < 0{,}62\sqrt{\frac{D^3}{\lambda}} \qquad \text{Eqn(3.1)}$$

λ is a wavelength and D is the biggest size of an antenna in the equation above. [12]

The near-field area is the reagent region between the near field and the far field. In this area the radiation field components are dominant, and the angular field distribution varies depending on the distance to the antenna. In an infinitely focused antenna, the near field sometimes referred as the Fresnel zone by the optical terminology.

$$0{,}62\sqrt{\frac{D^3}{\lambda}} < R < \frac{2D^2}{\lambda} \qquad \text{Eqn(3.2)}$$

Far field is the region where the angular field distribution is independent of the distance from the antenna. If the antenna has a maximum dimension (D), such that it is larger when compared to the wavelength, the far-field region is defined as;

$$R > \frac{2D^2}{\lambda} \qquad \text{Eqn(3.3)}$$

In an infinitely focused antenna, the far-field region is sometimes called as the Fraunhofer Region [12].

We can classify antennas in 3 categories according to their radiation pattern as Isotropic Antenna, Direction Dependent Antennas (Directional) and Direction Independent (Omnidirectional) Antennas.

Isotropic Antenna is a hypothetical antenna which radiates same power in all directions. In these antennas, the power density is equal in all directions on the same distance.

Gain and direction are closely related to antennas. Directivity depends on how an antenna directs its power density in one or two different directions. Because the total energy remains the same, but when the energy is pointed in a particular direction, the signal strength will increase. This increase in signal strength will also increase antenna gain. The antenna is called direction dependent when the power density is direction dependent in this way by concentrating radiation in a particular direction. The main beam lobe shows the direction in which the maximum radiation or signal is received. The lateral beam lobes and the posterior beam lobes indicate loss of energy and a good antenna design is required to minimise these lobes [13].

The omnidirectional antennas make equal radiation in all directions, and they called as direction independent because they do not radiate the power to any one direction. These antennas radiate the power like a directional antenna in one dimension (e.g. azimuth) like an isotropic antenna in another dimension (e.g. elevation). Therefore we can call this type of antennas as different kind of directional antennas [13].

3.1.2 Radiation Power Density

Electromagnetic waves are used for transmitting information from one point to another in a wireless way. Therefore, power and energy of the EM wave should be considered.

$$\vec{W} = \vec{E}\ x\ \vec{H} \qquad \text{Eqn(3.4)}$$

W is instant Poynting vector ($\frac{W}{m^2}$), E is instant Electrical Field Density vector ($\frac{V}{m}$), and H is instant Magnetic Field Density vector ($\frac{A}{m}$).

The Poynting vector we have mentioned means power density. If we take surface integral of Poynting vector, we can find the total power go through a closed surface.

$$P = \iint_S\ \vec{W}.ds = \iint_S\ \vec{W}.\hat{n}.da \qquad \text{Eqn(3.5)}$$

P: Instant total power; (W)

$\hat{n}$: unit vector;

da: the minimum surface in a closed area; (m^2)

$$\vec{E}(x,y,z,t) = Re[\vec{E}(x,y,z,t)e^{jwt}] \qquad \text{Eqn(3.6)}$$

$$\vec{H}(x,y,z,t) = Re[\vec{H}(x,y,z,t)e^{jwt}] \qquad \text{Eqn(3.7)}$$

$$\vec{W} = \vec{E}x\vec{H} = \frac{1}{2}Re\left[\vec{E}x\overrightarrow{H*}\right] + \frac{1}{2}Re\left[\vec{E}x\vec{H}.e^{jwt}\right] \qquad \text{Eqn(3.8)}$$

The Poynting vector with time average will be found as:

$$\vec{W}av(x,y,z) = \left[\vec{W}(x,y,z;t)\right]av = \frac{1}{2}Re\left[\vec{E}x\overrightarrow{H*}\right] \quad (\frac{W}{m^2}) \qquad \text{Eqn(3.9)}$$

Moreover, according to equation 3.9, the power density is:

$$P_{rad} = P_{av} = \iint_S\ \vec{W}.ds = \iint_S\ \vec{W}.\hat{n}.da = \frac{1}{2}\iint_S\ Re\left(\vec{E}x\overrightarrow{H*}\right).ds \qquad \text{Eqn(3.10)}$$

Isotropic antennas are making equal radiation in every direction. Because of this symmetrical spreading, the Poynting vector will not be a function of θ and Φ and only have an angular component.

Moreover, the power density is shown as:

$$W_0 = \widehat{a_r} W_0 = \widehat{a_r} \left(\frac{P_{rad}}{4\pi r^2}\right) \quad \text{Eqn(3.11)}$$

As we expected in the Isotropic antenna, the power density has a homogenous density around same radius r in a sphere according to Equation 3.11.

3.1.3 Radiation Intensity

Radiation intensity is defined as the power of the antenna per unit solid angle [12]. The intensity of the radiation is a far-field parameter and is calculated by multiplying the density of radiation by the square of the distance.

$$U = r^2 W_{rad} \quad \text{Eqn(3.12)}$$

U is Radiation Intensity, r is the distance and W_{rad} is radiation density. And radiation intensity depends on far region electrical field in this way :

$$U(\theta, \varphi) = \frac{r^2}{2\eta} \left|\vec{E}(r, \theta, \varphi)\right|^2 = \frac{r^2}{2\eta} \left[\left|\vec{E}_\theta(r, \theta, \varphi)\right|^2 + \left|\vec{E}_\varphi(r, \theta, \varphi)\right|^2\right] \quad \text{Eqn(3.13)}$$

$\vec{E}$: Far-field Electrical field intesity

$\vec{E}_\theta$, $\vec{E}_\varphi$: Far-field Electrical field intensity components

η: Characteristic empedance of the media

3.1.4 Directivity

The ratio of the radiation intensity in a given direction from the antenna to the radiation intensity averaged over all directions [12]. Mathematically can be expressed by this equation.

$$D = \frac{U}{U_0} = \frac{4\pi U}{P_{rad}} \quad \text{Eqn(3.14)}$$

We can express the maximum directivity in:

$$D_{max} = D_0 = \frac{U_{max}}{U_0} \quad \text{Eqn(3.15)}$$

D is Directivity, D_0 is maximum directivity, U is radiation density, U_{max} is maximum radiation density, U_0 is radiation density of the isotropic antenna, P_{rad} is the total radiated power.

3.1.5 Antenna Gain

One of the most critical parameters of an antenna is a gain determines the performance of the antenna and strictly depends on the directivity of the antenna. If we formulate the gain of antenna:

$$Gain = 4\pi \frac{Radiation\ Density}{Total\ Input\ Power} = 4\pi \frac{U(\theta,\varphi)}{P_{in}} = 4\pi \frac{U(\theta,\varphi)}{P_{rad}/v} \quad \text{Eqn(3.16)}$$

According to equation 3.17, the gain of an antenna equals to the multiplication of the directivity and the efficiency of the antenna.

$$G(\theta,\varphi) = v.D(\theta,\varphi) \quad \text{Eqn(3.17)}$$

v is the total antenna efficiency, $D(\theta,\varphi)$ is the directivity of the antenna. And we can represent the antenna gain in dB unit.

$$G_{dB} = 10\log_{10}(G(\theta,\varphi)) \quad \text{Eqn(3.18)}$$

Basic antenna parameters, especially antenna gain and directivity, are essential parameters for grasping antenna arrays and smart antennas.

3.2 Fundamentals of Antenna Arrays

When the radiation pattern of a single antenna is analysed, it is seen that the beamwidth is wide and the directivity is low. However, it is expected to concentrate the antenna power in the desired direction especially in the radar applications or when the distance between transmitter and receiver is long. A single antenna can meet this requirement, but only by increasing the power, in other words by improving the power of the electrical field which supported by antenna input power. However, the production of a single antenna to provide this power is difficult to assemble, and feeding of a single antenna which has this size is not practically feasible. These facts have been led to the design of antenna arrays. Several antennas are used together in certain geometries to provide the desired antenna

power. Antenna arrays are the antenna structures which are formed by combining several antennas in a certain geometric form.

Each of the array elements can be in different structures and different electrical properties. However, regarding ease of operation, each element is considered identical. Antenna arrays can be one or two dimensional. Each of these antenna elements radiates electromagnetic power to a specific point of space, and the total radiation of the array at that point is the sum of the radiations of each element. For that reason, a different radiation pattern than the radiation pattern of a single antenna element will be generated by the antenna array.

3.2.1 Linear Antenna Array Geometry

The simplest and most practical of antenna arrays are linear antenna arrays which consist of antenna elements placed on a line. This array geometry is shown in figure 3.1.

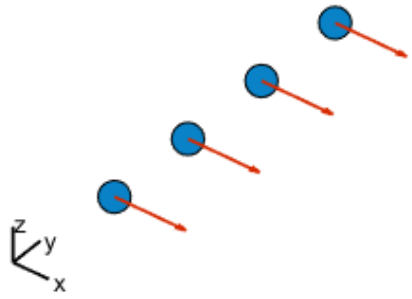

Figure 3.1: Linear Antenna Array

The simplest form of the linear antenna arrays is two element antenna array. The product of the electric field and the array factor of the array elements at the selected reference point gives us the total electric field generated at that reference point.

$$E(total) = [E(Effect\ of\ single\ element\ on\ the\ reference\ point) x Array\ Factor]$$

Eqn(3.19)

Each antenna series has its array factor. This array factor is usually expressed as a function of the number of array elements, the geometry of the array, the distance between elements, the phase and the amplitude.

Assume that the distance between two equivalent dipoles is d, the phase difference is β, and there is no coupling between the elements, the electric field formed by the array at point P is:

$$E_T = E_1 + E_2 \qquad \text{Eqn(3.20)}$$

$$E_T = \widehat{a_\theta} j\eta \frac{kll_0}{4\pi}\left[\frac{e^{-j[kr_1-(\beta/2)]}}{r_1}\cos\theta_1 + \frac{e^{-j[kr_2-(\beta/2)]}}{r_2}\cos\theta_2\right] \qquad \text{Eqn(3.21)}$$

If we think we are far away from the observation point, we can assume $\theta_1 \cong \theta_2 = \theta$ and:

$$r_1 \approx r - \frac{d}{2}\cos\theta \qquad \text{Eqn(3.22a)}$$

$$r_2 \approx r + \frac{d}{2}\cos\theta \qquad \text{Eqn(3.22b)}$$

$$r_1 \cong r_2 = r \qquad \text{Eqn(3.22c)}$$

If we reorganise equation 3.22 according to last equations:

$$E_T = \widehat{a_\theta} j\eta \frac{kll_0 e^{-jkr}}{4\pi r}|\cos\theta|\left[e^{+j(kd\cos\theta+\beta)/2} + e^{-j(kd\cos\theta+\beta)/2}\right] \qquad \text{Eqn(3.23)}$$

$$E_T = \widehat{a_\theta} j\eta \frac{kll_0 e^{-jkr}}{4\pi r}|\cos\theta|\overbrace{2\cos[\tfrac{1}{2}\cos kd\cos\theta + \beta]}^{\text{AF}} \qquad \text{Eqn(3.24)}$$

And according to this equation, the normalised array factor is:

$$(\mathrm{AF})_\mathrm{n} = \cos[\tfrac{1}{2}\cos kd\cos\theta + \beta] \qquad \text{Eqn(3.25)}$$

And this array factor is only valid for the array we have analysed. If we expand antenna array analysis from two-element linear array to n-elements linear array, the linear array geometry which has M=2N elements is shown in Figure 3.2.

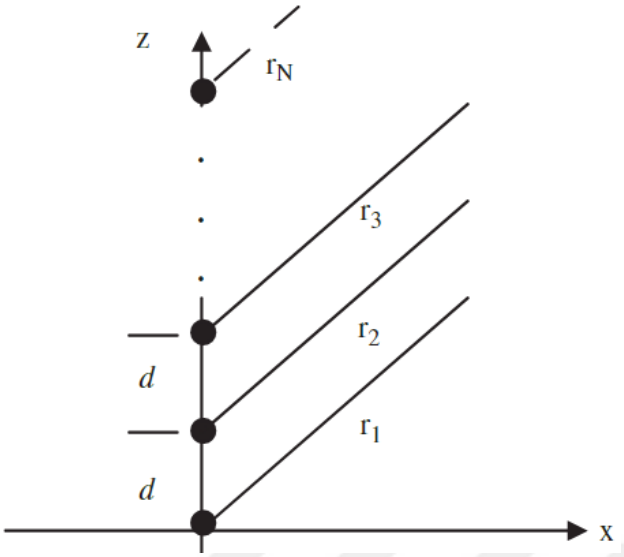

Figure 3.2: Linear Antenna Array Geometry with N-Elements [14]

Assume that all the elements in the array are identical and that there is β degree phase difference between them, In this case, the electrical field expression for array elements through +z direction is:

$$E_T = a_1 e^{j\left(\frac{1}{2}\right)kd\sin\theta)} + a_2 e^{j\left(\frac{3}{2}\right)kd\sin\theta)} + \cdots + a_N e^{j\left(\frac{2N-1}{2}\right)kd\sin\theta)} \quad \text{Eqn(3.26)}$$

$$E_T = \sum_1^N a_n e^{j\left(\frac{2n-1}{2}\right)kd\sin\theta)} \quad \text{Eqn(3.27)}$$

And it should be complex conjugate of equation 3.27 in –z-direction:

$$E_T = \sum_{n=1}^N a_n e^{-j\left(\frac{2n-1}{2}\right)kd\sin\theta)} \quad \text{Eqn(3.28)}$$

Therefore array factor for the array shown in Figure 3.2 will be:

$$AF(\theta) = 2\sum_{n=1}^N a_n \cos\left[\frac{(2n-1)}{\lambda}\pi d\sin\theta\right] \quad \text{Eqn(3.29)}$$

3.2.2 Planar Antenna Arrays

Planar antenna arrays are formed by placing antenna elements on a plane. The planar antenna array is shown in Figure 3.3:

The most important advantage of planar antenna arrays over linear antenna arrays is that the radiation pattern can be scanned in two dimensions (in the angular axes θ and Φ). In other words, while linear arrays can sweep their radiation pattern in one dimension, planar antenna arrays can sweep the beam in two dimensions. It means planar antenna arrays

can be used in three-dimensional space properly. Therefore planar antenna array structure is suitable to use in Automatic Antenna Rocket Tracking System.

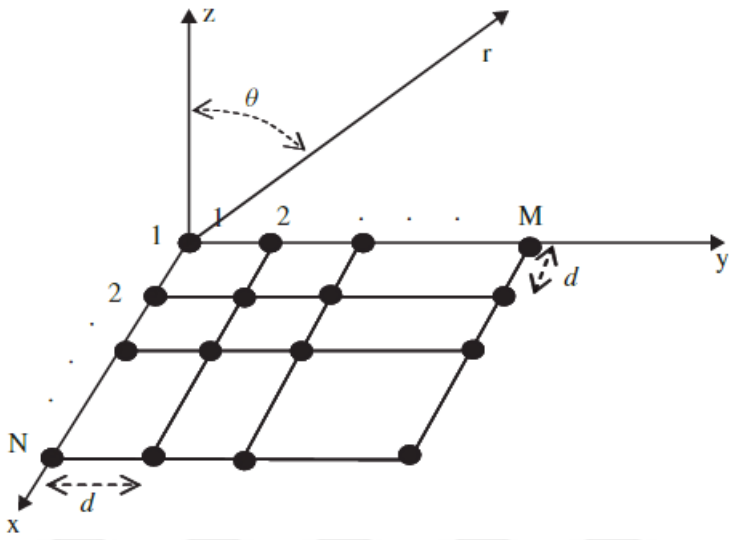

Figure 3.3: Planar Antenna Array Geometry with MxN-Elements [14]

We can generate the formulation of the array factor for the planar array which has MxM antenna elements. Firstly if we think there are M elements in the x-direction with same separation, we can find array factor with [1]:

$$AF = \sum_1^M I_{ml} e^{j(m-1)kd_x \sin\theta \cos\emptyset + \beta_x} \qquad \text{Eqn(3.30)}$$

I_{ml} is stimulation coefficient, dx is a distance between antennas on x axis and β_x is the phase difference between them. When we also place antenna elements on y-axis in dy distance and β_y phase differences as we placed for x- dimension we will be designed a planar antenna array with MxM elements. In this case, we can evaluate the array factor formulation in this way:

$$AF = \sum_1^n I_{1n} \left[\sum_1^M I_{m1} e^{j(m-1)kd_x \sin\theta \cos\emptyset + \beta_x}\right] e^{j(n-1)kd_y \sin\theta \cos\emptyset + \beta_y} \qquad \text{Eqn(3.31)}$$

In here the amplitude coefficient for (m,n) element is:

$$I_{mn=} I_{1n} I_{m1} \qquad \text{Eqn(3.32)}$$

If we accept amplitude coefficient is homogeneous, $I_{mn=} I_0$, we can re-write the array factor equation as:

$$AF = I_0 \sum_1^M e^{j(m-1)kd_x \sin\theta \cos\emptyset + \beta_x} \sum_1^n e^{j(n-1)kd_y \sin\theta \cos\emptyset + \beta_y} \quad \text{Eqn(3.33)}$$

3.2.3 Antenna Geometry and Sequence of Antenna Elements

When we look at the array factor terms, it can be said that these expressions depend on the distance between the elements. If the distance between the elements is greater than the half-wave (λ/2) value, then there is a reduction in performance of the antenna array. On the other hand, when the distance between the array elements is less than (λ/2), it is observed that the main ear and the side beams expand when the array radiation pattern is examined. Therefore, choosing the distance between elements as λ/2 is widely used in practical applications.

Furthermore, for tracking the telemetry signal, firstly we should estimate the direction of arrival of the signal. Especially, for our application, if the distance between antenna elements is bigger than half of the wavelength, phase ambiguity problem occurs due to the periodic nature of the telemetry signal. Also, the reduction in the efficiency of antenna array will be observed. However, the antenna elements in tracking station have high gain and directivity (18 dBi). It means when we place them in the distance closer than λ/2, mutual coupling effect will be catastrophic for gathering the signal. Moreover, the telemetry communication signal will be in broadband, and it is working in ISM 2.4 GHz band. In the shortest case the half of the wavelength will be:

$$\frac{\lambda}{2} = \frac{\mathrm{c}}{2\mathrm{f}} = \frac{\mathrm{c}}{2\mathrm{x}2.4835\ \mathrm{GHz}} \approx 6\mathrm{cm} \quad \text{Eqn(3.33)}$$

The diameter of antennas is not appropriate to place antennas closer than half of the wavelength. We will analyse deeper how the distance between elements affect the performance of the tracking system in the next chapter.

3.3 Fundamentals of Smart Antennas

The most important part of the system which makes it smart is digital signal processing capacity. Although this technology is known as a new technology, its foundations are based on the 1970s and 1980s. Smart antennas were first used in military applications [13] Especially; they have used as a countermeasure against electronic signal mixers on EWF (Electronic Warfare). Also, the smart antennas also were used in military radar systems in World War II. Nowadays, smart antenna systems are also used in commercial fields by using low-cost signal processing processors. The increasing popularity of mobile communication systems and the increase in the number of users in the last years has

increased the capacity requirement and necessity a good service quality. The conditions limiting the capacity and service quality in mobile communication systems are examined under three main groups:

- Multipath Attenuation
- Propagation Delay
- Interference

Smart antennas are used, to solve these problematic effects in mobile communication systems. Multipath attenuation is one of the most critical effects in mobile communication. Any advancement in this attenuation makes great advantage for GSM systems. Furthermore, the ability to direct the antenna beam in determined direction reduce the possibility of interference and enhance the channel capacity and performance by that way. We can make an analogy with a human ear to understand smart antennas better. People can position an object moving around, even in a dark environment or when their eyes are closed, thanks to the sound which the target removes, and can detect the distance of an incoming sound. This is done in 3 steps: The sound waves are detected by ears, Due to the distance between ears the sound wave has been detected in time delay in a different ear. The brain of the human process the information and estimate the direction and location of the sound source [13].

Smart antenna systems are the same systems that use two antennas instead of two ears and a processor instead of a human brain. That is, the time-delayed signals processed by the antennas can be processed by a processor to estimate the arrival angle, suppress undesired signals, or intensify the power in the desired direction.

Smart antennas can be classified into two groups as “switched beam” and “adaptive array systems”. In the presence of a low level of interference, both types of smart antennas make significant gains compared to conventional systems. Nevertheless, when there is a high level of interference, adaptive systems provide significantly greater coverage than conventional systems or switched-beam systems due to the ability to reject interference. Adaptive antenna arrays ensure that the main user signal is maximized and common channel interference signals are suppressed at the highest level. However, this success of adaptive antenna systems requires a more complex structure and higher cost.

3.3.1 Adaptive Antenna Arrays

Adaptive antenna systems are not only limited to placing the user signal at the maximum point of the main ear but also completely suppress common user interactions. We can see that property of smart antennas in Figure 3.4.

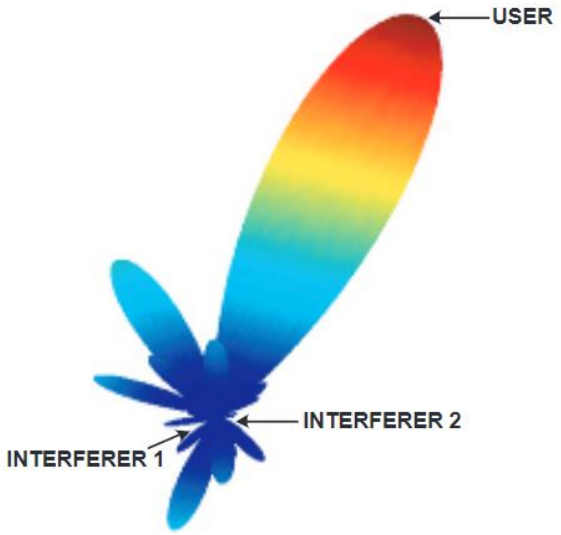

Figure 3.4: Representation of the Adaptive Array Coverage [13]

In addition, it can provide a wide range of coverage, because it can control the whole radiation pattern. Adaptive systems can find and track signals and increase signal reception while suppressing other interferences by using digital signal processing.

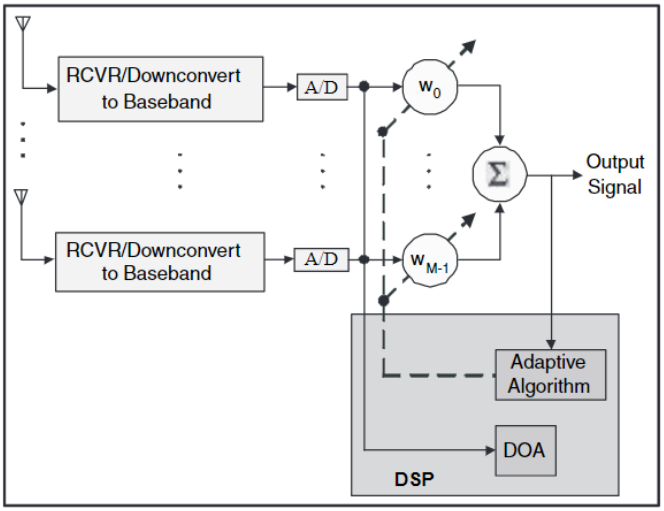

Figure 3.5: Functional Block Diagram of Adaptive Array Systems [13]

As shown in the Functional Block Diagram, the data received from the array elements are sent to the DOA (Signal Arrival Angle), where the time shift between the data received from the array elements is calculated, and the signal arrival angle is calculated. The adaptive algorithm then calculates the appropriate weight functions for the optimal radiation pattern by using the cost function. Adaptive antenna systems are much more costly than switched-antenna systems because they use sophisticated digital signal processing methods.

Adaptive antenna systems use sophisticated digital signal processing methods to estimate DOA of the target signal and for differentiating the multipath signal from the interference signal. MUSIC and ESPRIT are some examples of them. MUSIC and ESPRIT algorithms are explained in the fifth chapter.

Two primary methods have been identified for adaptive antenna systems. The first one is based on prior knowledge of the desired signal. This known signal is then compared to the received signal, and the weight vector is adjusted such that the MSE (mean square error) between the known signal and the received signal is minimised. At this point, the 0's in the radiation pattern can be set to correspond to the interference. Since the weight values are shaped according to the incoming signal, the multipath attenuation is reduced as well as the suppression of interference signals.

In the second method, the arrival angle of the signals transmitted from all signal sources to the antenna array is first defined. The complex weight parameters are set according to there is maximum directivity to the target and minimum directivity (0's of the pattern) to the interferences [15]. It can be seen that this method is lacking in practical applications where there are too many signal arrival angles, such as multipath. Furthermore, the possibility of error in estimation is too high.

Another important advantage of adaptive antenna systems is that they have a shareable spectrum. Thanks to the system's accurate tracking and strong interference suppression capability, many users can share the same channel in the same cell. When there is a moving user, the radiation pattern is constantly updated to fix this position.

3.3.2 Switched Beam Antenna Arrays

Switchable antenna systems are the simplest antenna systems among smart antennas. It consists of a structure that is formed from constant rays that are oriented in certain directions. Such a system first measures the signal strength, selects one of the predetermined fixed spins, and switches the mobile phone by switching from one mode to another as the mobile phone moves. (Figure 3.6)

Instead of creating a directional antenna pattern using metallic structures and the physical design of a single element, switched-off antenna systems use a combination of their outputs, taking advantage of a number of components to achieve a finer directional antenna pattern and signal than a single antenna element.

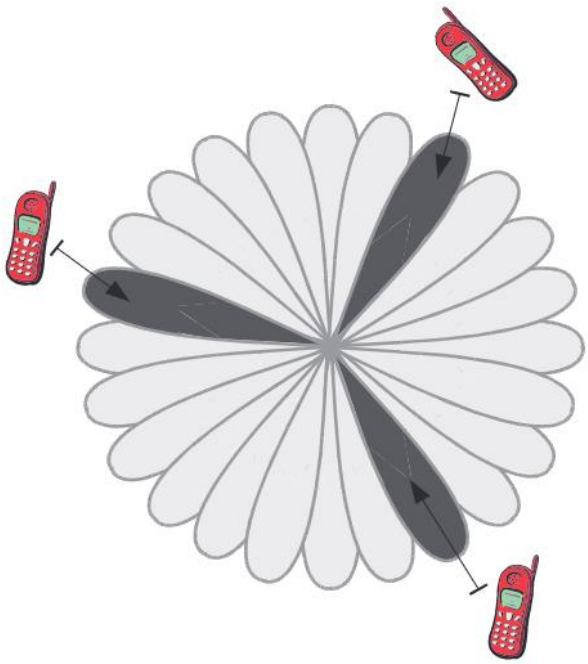

Figure 3.6: Switched Beam Coverage Pattern [13]

3.3.3 Structure of Smart Antennas

Intelligent antenna systems consist of antenna arrays that shape the radiation pattern and a processor that allows the radiation pattern to be shaped and directed. The adaptive antenna system consists of four main parts: Antenna Array, RF Converters, Beam Formers, Demodulator.

The antenna array consists of N antennas. Each element generates a single output signal by combining the arrival signals. This signal is converted to digital signal by RF (Radio Frequency) Converter. The beam shaping unit determines the complex weight vectors and multiplies these weight vectors by the arrival signals from each array element. Via this way, the antenna radiation pattern is formed. As can be seen in the previous sections, these antenna systems can perform both magnification and suppression. The radiation pattern obtained from the beamformer is optimized according to the largest construction of the signal from the desired user or the suppression of interference signals.

This intelligent antenna system, consisting of N array members, has the ability to distinguish at most N-1 signals, but this value varies due to multipath points. Calculations in the beam shaping unit are a kind of digital signal processing. In this unit, there is a processor-based unit on which the DOA estimation algorithm runs.

Each wireless system consists of receiver and transmitter parts. However, these two parts are of greater importance in smart antenna systems. This is because it is essential that

the receiver and transmitter sections work in coordination with one another in the operation of intelligent antenna systems.

3.4 Evaluation of Smart Antenna Systems

The birth of smart antenna systems has led to many changes and developments, especially in mobile communications, both civilian and military. In addition to providing increased performance of many systems with intelligent antennas, the cost factor is also an important parameter that is changing. This section discusses the benefits and drawbacks of smart antenna systems.

With the emergence of smart antennas, these systems have greatly influenced the performance of cellular networks. The benefits of intelligent antenna systems and the innovations it brings to mobile systems will be as follows;

- Enhancement Capacity
- Enhancement of Communication Range
- New Services
- Security
- Enhancement in SIR (Signal-to-Interference Ratio)

The impact of intelligent antenna systems regarding spreading and planning of mobile systems is considerable. in particular, enhancement in the capacity and range increases the interest in smart antenna systems. In densely populated areas, the main source of the noise is the interferences from other users. Along with the development of adaptive systems, substantial improvement has been achieved in the strength of the received signal and the reduction of the interference signal levels and in this respect the SIR. Furthermore, when smart antennas are used, spatial information about the user becomes available to reach. The position of the user can be determined more precisely than the other systems. Positioning can be used in many different applications, such as locating emergency calls.

Even though, there are many advantages of smart antenna systems they also have some disadvantages.

- Cost Factor
- Complexity in Antenna Structure

Even though the physical appearance of smart antenna systems is similar to that of conventional antennas, smart antenna systems have a much more complicated structure. Especially if adaptive antenna arrays are used, the beam shaping process requires intensive processing. Therefore, the base stations which use the smart antenna system must contain potent numerical processors and control systems. For this reason,

undoubtedly, base stations installed with a smart antenna system are much more costly than traditional base stations.

4 Literature Review of Direction of Arrival Estimation Methods

The direction of arrival (DOA) estimation is a topic of signal processing which tries to estimate the direction of Radio Frequency (RF) signals received by the receiver antenna or antenna array. If the telemetry signal comes to the two different antenna for every tracking dimension, automatic antenna tracker can estimate the direction of the rocket. After estimation of the angle of arrival of the telemetry signal, the tracking controller can define the error angle and can move the antenna to reach the line of sight communication. Numerous studies have been conducted to estimate the DOA. The methods for determination of the direction datum of RF signals can be analyzed under three classes, the classical, the monopulse and the subspace methods [5]. The classical methods are based on a scanning antenna beam over the space where target`s presence is suspected [4]. Therefore, tracking antennas normally have high directivity to increase tracking range and suppress the signals coming from different RF sources.

4.1 Classical Methods

The class of classical methods contains two groups, “Single Target Tracking” and “Multiple Target Tracking” [5]. There are two different classes of single target tracking groups, which are scanning methods and monopulse methods. There are two scanning strategies, Sequential Lobing which is the oldest method and Conical Scan.

4.1.1 Sequential Lobing Method

In sequential lobing, a tracking antenna array is enlightening two symmetric predetermined positions under the line of sight sequentially by switching. Due to the accuracy of the tracking system is also limited by switching noise of the system. The tracker measures two signal levels and computes angular error signal. This tracking mechanism needs four antennas to scan in 2-Dimensions [5]. Even though this method is easy to implement, it is too noisy and slow for our project case. Figure 4.1 is illustrating sequential lobing mechanism when the target is on tacking axis.

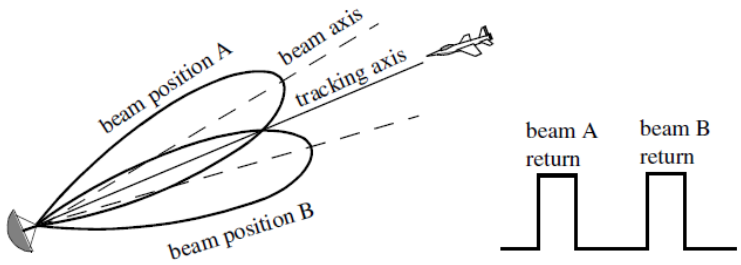

Figure 4.1: Sequential Lobing Method [5]

4.1.2 Conical Lobing Method

The Conical scan method was developed to avoid switching noise limitation of sequential lobing and also some of the DoA systems are still using this system. This scanning mechanism uses a rotating antenna beam around tracking axis in $\omega_s$angular speed. The angle between the beam axis (Line of Sight) and tracking axis called as “squint angle” [5]. Figure 4.2 is illustrating Conical Scanning mechanism.

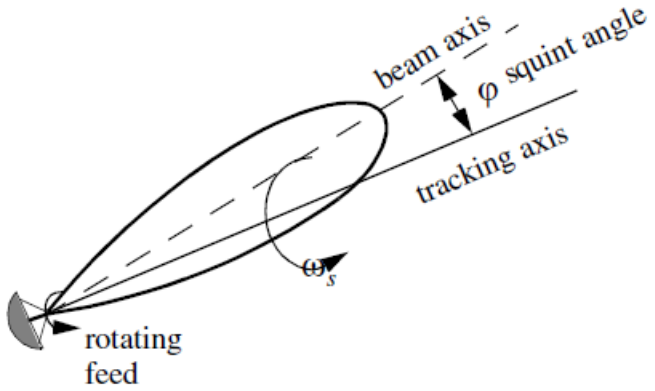

Figure 4.2: Conical Scanning Method [5]

Figure 4.3 shows the simplest conical scan radar system. The reason for using the envelope detector for antenna tracking control is the nature of its output signal in the case when the target is within tracking range. When the target is on the tracking axis, the output signal has E_0 amplitude. However, if the target is on the beam axis, we get the maximum amplitude when the beam illuminates the target. And likewise a minimum amplitude is received when the beam illuminate empty space. For the reason of that, the output signal of mixer and IF amplifier block is in the waveform of AM modulated signal. Radar system use Automatic Gain Control to control return signal strength [5].

The scan rate of the mechanism is limited by a mechanical or electronic scanning method. Although electronic scanning is faster than mechanical, electronic scanning needs very sensitive phase controllers. The squint angle should be large enough to get better error signal because the SNR suffers when the target is on the tracking axis due to the equal drop in the antenna gain [5].

Scanning techniques simply add harmonic movements to the original antenna reference becoming simpler and cheaper compared with other methods. These movements cause a variation of the received signal. The analysis of the received signal allows estimating the beam pointing deviation [10].

Except for scanning methods, there are monopulse methods for estimating the direction of arrival of the RF signal. Monopulse methods will be analyzed under three titles which are

“Amplitude Comparison”, “Phase Interferometry” and “Time Difference of Arrival” (TDOA). All these methods need minimum two antennas per dimension. To track our payload we need 2-Dimensional tracking because minimum four antennas should be used in the tracking system.

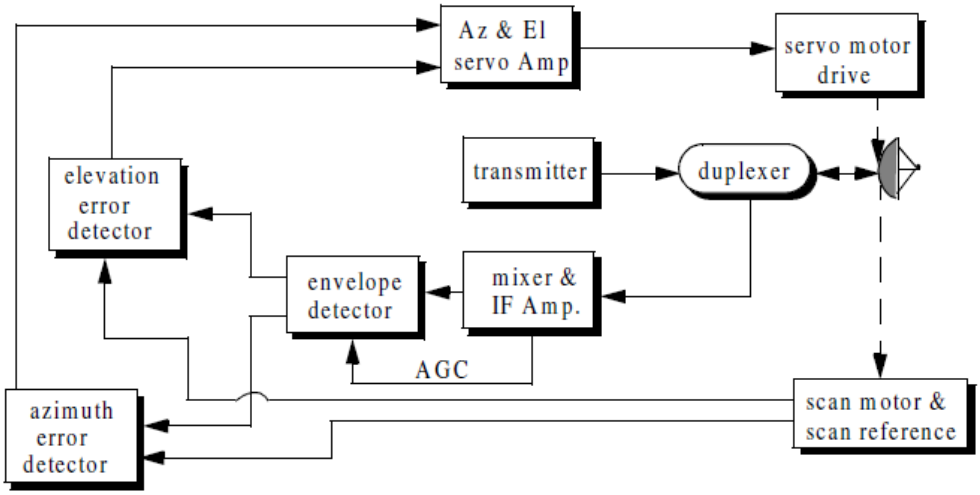

Figure 4.3: Simplified Conical Scanning Radar [5]

4.2 Monopulse Systems

4.2.1 Time Difference of Arrival Method

The time difference of arrival method (TDOA) measures the difference in arrival time of one signal at multiple antennas to calculate the DoA and range the emitter. The accuracy of the TDOA method depends on the distance between antennas. The TDOA method of direction finding has the potential to be very accurate and yields location in addition to direction; however, its heavy reliance on accurate measurements creates problems in small-scale systems. To achieve reasonable requirements, the distance between the antennas should be the order of the kilometres. Due to the second ground station has a compact configuration, this method is not applicable to our case [6].

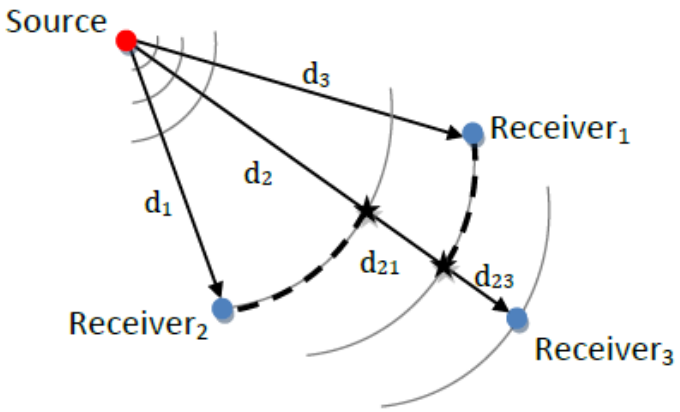

Figure 4.4: Geometry of a TDOA system [7]

4.2.2 Amplitude Comparison Method

The amplitude comparison method uses two or more directional antennas pointed in different directions that the ratio of the gains for the two antennas will be unique for each angle within the field of view. The system calculates the DoA by comparing the amplitude ratio of the signals received by the two antennas that have a known gain pattern. According to work of Silva et al. [7], the amplitude comparison method can have an accuracy of up to four degrees that is fatal for a tracking system that uses highly directional antennas.

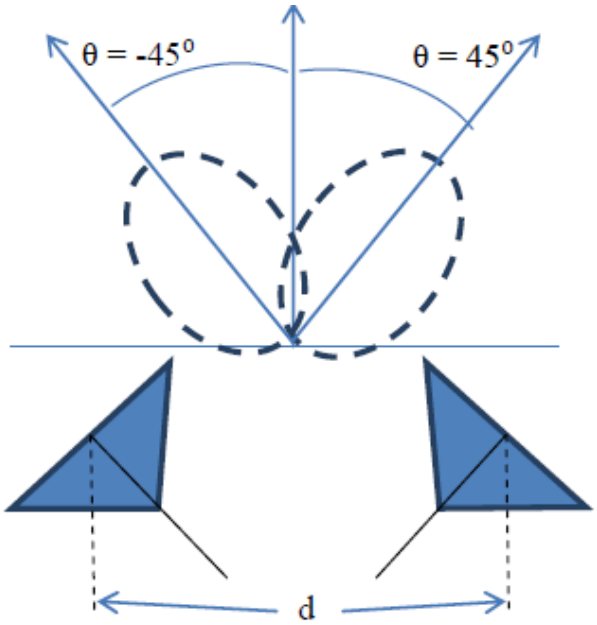

Figure 4.5: Two-antenna system for amplitude comparison method [7]

If we consider the noise of the environment, the amplitude of the received signal is affected by noise more than the phase of the signal. Because of this fact, phase comparison method`s noise immunity is better than amplitude comparison methods.

One of the most widely used method in amplitude comparison DOA estimation category is Watson-Watt direction finding method. In this method, Adcock or loop antenna is used as an antenna structure. Loop antennas used for finding the direction of lower frequencies RF signals because of their compactness. However, for higher frequencies more efficient antenna structures should be used. Therefore, Adcock antenna structure used for higher frequencies. In an **Adcock array**, the four antennas are grouped in pairs, laying each pair along with a reference axis to create a figure-of-eight azimuthal gain pattern by the difference of the reciprocal antennas' voltages [18, 19]. The voltages of a pair of antenna elements' should be subtracted vectorially for generating x-axis voltage and the voltages of the other pair of antenna elements' should be subtracted vectorially for generating y-axis voltage. DOA of the RF signal is estimated by using these measurements [20].
Even though, Watson-Watt method is the forerunner of DOA estimation techniques. Other methods are used in tactical applications due to their superior performance. For instance, Phase comparison methods have many advantages over Amplitude comparison methods (i.e. Watson-Watt) due to the amplitude of the data is more susceptible than the phase of the data while transferring over atmosphere.

4.2.3 Phase Comparison Methods

We can classify phase comparison methods in two, Doppler methods and Interferometer method.

4.2.3.1 Doppler Method

The Doppler method is inspired by famous physical fact called as Doppler Effect. The Doppler effect is observed whenever the source of waves is moving with respect to an observer. The Doppler Effect can be described as the effect produced by a moving source of waves in which there is an apparent upward shift in frequency for observers towards whom the source is approaching and an apparent downward shift in frequency for observers from whom the source is receding. As an example, It may have noticed that when an ambulance or police car goes past, its siren is high-pitched as it comes towards the observer, then becomes low-pitched as it goes away. Imagine we have a single antenna mounted on a rotating disk. As this disk is rotated, the antenna will move closer to and then further away from the transmitter. At positions A and C, the antenna is stationary relative to the transmitter, so Doppler shift = 0 At position B (moving away) and D (moving towards), Doppler shift will be maximum. Continuous measurements of Doppler shift will yield a so-called Doppler sine-wave. By making frequency shift measurements as we go around the wheel (so to speak), we get a Doppler sine wave with two zero crossings at A and C, i.e. where there is no Doppler shift. The second zero crossing

(downwards slope) is the point closest to the transmitter. This sine wave has the same frequency as the rotational frequency (ω) of the antenna [21].

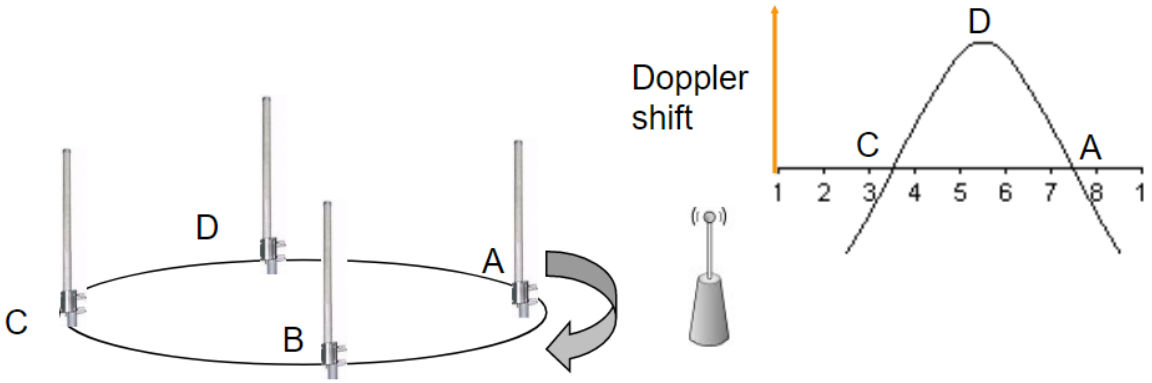

Figure 4.6: Doppler Direction Finding method [21]

The only difference is the phase differences of the tones. This phase difference is used to determine the angle of arrival [22,23]. However, there are many disadvantageous of Doppler RDF (radio direction finding) method like mechanical difficulties and effects of rotating antenna. Therefore, Psuedo-Doppler method has been developed to solve these problems, and most of the RDF systems use Doppler Methods are in Psuedo-Doppler Method now. The Pseudo-Doppler direction finding method is a phase comparison DF method that depends on the phase differences of the antenna elements which are circularly placed. As mentioned above, the frequency shift caused by the Doppler effect can be determined by rotating an antenna mechanically and then, the direction of arrival can be calculated by using this frequency shift. In the Psuedo-Doppler Method, the Doppler Frequency shift is created by switching the receiver antenna of the antenna array which is equally and circularly disposed (Equally and circularly placement of the antennas is for easy implementation of the Pseudo-Doppler method). The frequency of the incoming wave signal suddenly changes at the switching instants. This frequency shift is the phase differences between the antennas. The output of the switching circuitry feeds an FM demodulator. By using the information gained from the FM demodulator output, phase differences between adjacent antennas can be determined and used to determine the incident waves' direction of arrival [20, 24].

4.2.3.2 Interferometer Method

In the literature, interferometer and phase interferometer methods refer to the same method. The interferometer method relies on the phases of the incident wave signal at

different antennas. Since the Pseudo Doppler method also depends on the phases of the received signal at distinct antennas, the Pseudo Doppler method is also accepted as single channel implementation of the interferometer method [20].

Interferometer-based DF systems have many advantages over other DF systems, including better accuracy, high bandwidth, and higher speeds. Moreover, while all DF systems suffer from multi-path effects caused by the environmental conditions, like reflection off towers, buildings, power lines and other structures, the interferometer method minimises these effects by using wide aperture antenna arrays [20, 22]. In this chapter, we will only mention the Conventional Interferometry method. Correlative Interferometry method will be explained in detail in chapter five.

Phase interferometry, like TDOA, relies on the time delay of the arrival of the signal between two or more antennas. Instead of measuring the time of arrival phase interferometry method measures phase difference between antennas. Unlike the TDOA the phase difference can be measured accurately over short antenna distances [6]. An antenna array consisting of three or more antennas that are arranged horizontally at an appropriate distance is used as the antenna system of an interferometer DF System. The outputs of these antennas are connected to phase coherent identical receiver system. The phase coherency of the receivers may be the most critical point in implementing a phase dependent DF system. This receiver system takes RF signals from antennas and converts them to a lower Intermediate Frequency (IF) for ease of processing. The outputs of the phase coherent receiver systems are fed to the DF processor that first determines the phase differences between the signals and then calculates the angle of arrival of the incident wave signal [10, 6].

Assume the distance between the two antenna is “s” and the distance from the RF source to antenna1 (A1) is “d1” and to antenna 2 (A2) is “d2”. If “d1” and “d2” is much bigger than the “s”. We can assume “d1” and “d2” as parallel. Figure 4.7 is illustrating two antenna phase interferometry systems geometry.

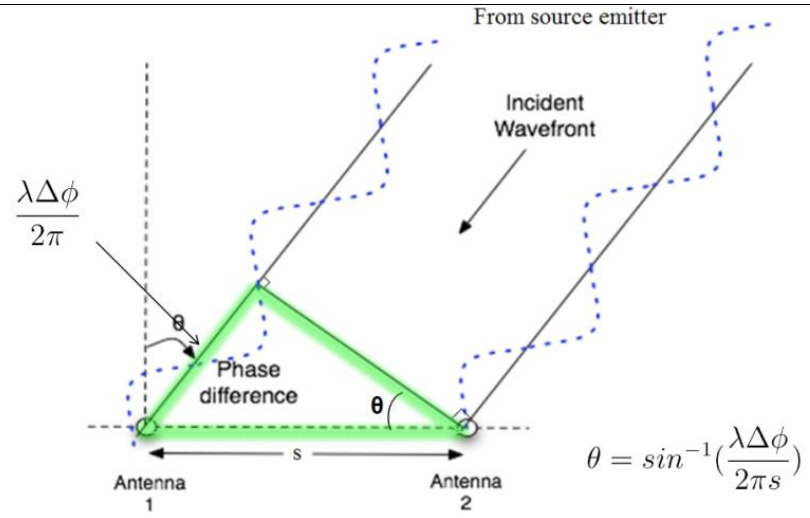

Figure 4.7: Two-antennas phase interferometry systems geometry [6]

In this case, the distance between p and A2 manages the phase difference between this two antennas.

$$\Delta\varphi = \frac{(2\pi s)}{\lambda}\sin(AoA) \qquad \text{Eqn(4.1)}$$

$$\sin(AoA) = \frac{\Delta\varphi * \lambda}{2\pi s} \qquad \text{Eqn(4.2)}$$

Even though, the accuracy of phase interferometry system is increased by the distance between antennas as TDOA method. The phase difference cannot be distinguished by these equations if the antenna separation distance is bigger than half of the wavelength due to the multiple solutions of it. This ambiguity can be solved by separating antennas closer than half of the wavelength. However, in that case, the accuracy of the system will be suffered. The meaning of small antennas means small aperture and low gain. Therefore, a different approach should be established to solve the issue. The source of ambiguity comes from the distance of pA2 longer than the wavelength. This adds one more unknown integer parameter to our equation. Elimination of this extra parameter can be done by adding one more equation to the system, and the meaning of this is adding the third antenna to the system [6].

To find DOA, firstly, phase difference should be calculated between antennas 1-2 and 1-3. Secondly, Phase differences which are calculated will be used in finding unambiguous DOA. The final calculation is performed by using the phase difference between antennas 1-3 as the larger separation.[6] If the “i” is the unknown integer:

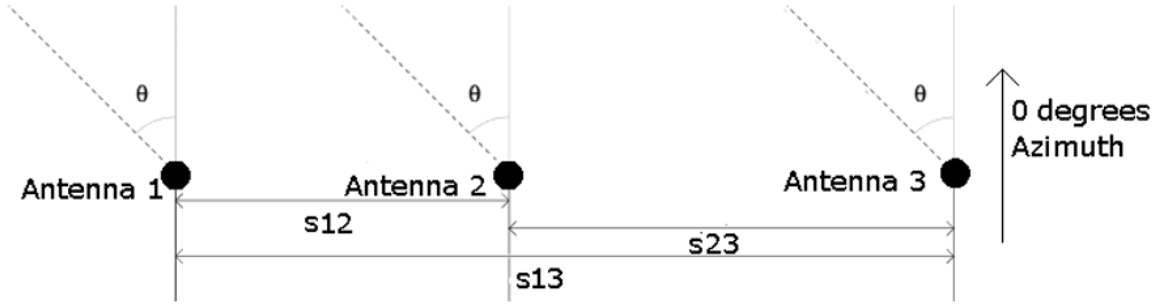

Figure 4.8: Three-antennas phase interferometry systems geometry [6]

$$\Delta\varphi_{12} + i_{12} = \frac{s}{\lambda}\sin AoA \qquad \text{Eqn(4.3)}$$

$$\Delta\varphi_{13} + i_{13} = \frac{s}{\lambda}\sin AoA \qquad \text{Eqn(4.4)}$$

Therefore

$$\Delta\varphi_{13} = \frac{s_{13}}{s_{12}}\Delta\varphi_{12} + \frac{s_{13}}{s_{12}}i_{12} - i_{13} \qquad \text{Eqn(4.5)}$$

For every i_{12} and i_{13}solutions yield a line representing a set of possible phase differences.

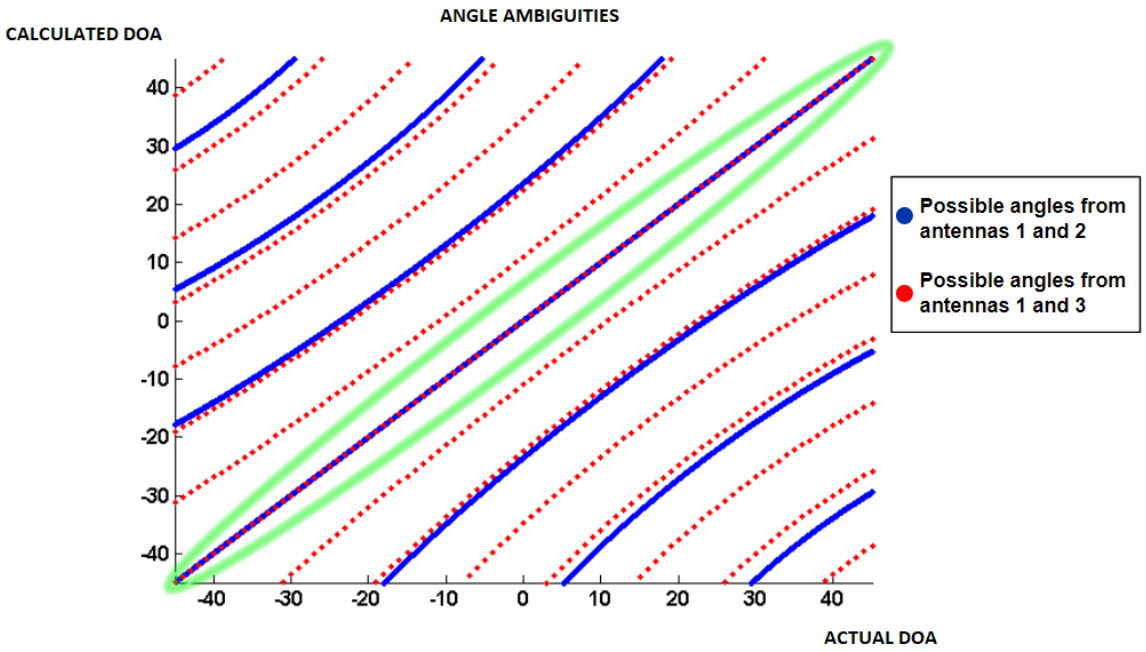

Figure 4.9: Solutions Lines of Phase Ambiguity Solution Technique [6]

Blue and red lines in Figure 4.9 represent all the solutions when there is no noise in the system. However, when the noise is added, a solution of the equation be equal to the

neighbourhood of lines. The nearest line is chosen as a result of DOA calculation in that case.

The true phase is determined by $\Delta\varphi 2\pi + I2\pi$, where $\Delta\varphi$ is the normalized measured phase difference I is the number of full phases as determined in Figure 4.9. noise of confidence is shown with green line, then the system is confident that it has resolved the phase correctly. Increasing the confidence range raises the possibility that the system will confidently report the incorrect angle while reducing it raises the possibility of reporting a correct result as uncertain. [6]

If there is high-level of the noise, the measured phase can bounce between two or more possible true phases. For solving this problem, a history of calculated angles can be saved to the memory to help determine which angles to use. For a fast moving target as we track it is not possible due to the calculation time. Adjacent lines of true phase will yield drastically different results for DOA because moving over one line represents changing the phase difference by 2π radians, so it can be quite clear when noise causes the calculation to choose the wrong phase line. This risk can be solved by choosing the antenna spacing such that there is the greatest possible distance between true phase lines. In an ideal, noiseless environment the measured phase will always appear on one of the true phase lines. When the lines are far apart, the noise has to corrupt the phase measurement by more before it resolves to an incorrect angle. The worst case scenario occurs when two incident true phase lines are generated by Equation 4.5. In this case, there will always be two completely ambiguous results for a certain set of measured phases. If the needed reliability cannot be achieved through optimal spacing and noise reduction, the field of view can be limited to reduce the total number of lines [6].

4.3 Subspace Methods

The techniques which used vary depending on whether the source is one or more. In the case of there is only one signal source, we can use the phase difference between the two elements of the antenna array and efficiently predict the arrival angle.

However, tracking multiple targets needs a different approach. Because every target sends telemetry signals randomly and the signals reach to the antenna elements at different times. In this case, the direction of arrival algorithms such as Capon Method designed in 1969 which is a reorganisation of Maximum Likelihood Method(ML) for DOA problem [16]. From the mid-1970s, subspace estimation techniques began to be used. Pisarenko (1973) opened a new era in this area by first modelling the noise-containing system with the approach of covariance. Later, a measurement model, which is independent of the geometry of the sensor arrays, was developed by Schmidt (1977), and it called MUSIC (Multiple Signal Classification) methods [16].

Even though the MUSIC method is widely used and can find DOA with very low error angles, It has to scan all parameter space. This makes MUSIC algorithm computationally heavy. For the sake of solving this problem, ESPRIT (Estimation of Signal Parameters via Rotational Invariance Techniques) method has been developed [17]. With this method, it is possible to estimate DOA without scanning all parameter space, and the computation and the storage costs due to the MUSIC method are reduced by this way.

4.3.1 MUSIC Algorithm

The MUSIC algorithm is a high-resolution multiple-signal classification method that uses the eigenvalues of the input covariance matrix [25, 26]. The number of signals, DOA, the power of incoming signals and cross-correlations between them, and the noise power can be estimated by MUSIC Algorithm [26]. The standard MUSIC (Multisample Classification) Algorithm was developed by Schmidt.

4.3.1.1 Data Model

For signal arrival estimation, primarily a signal model should be constructed. For a linear antenna array with M identical, isotropic antennas, the total signal from the D signal sources in the far field region can be expressed by the following relation.

$$u(t) = \sum_{i=0}^{D-1} a(\varphi_i) S_i(t) + n(t) \qquad \text{Eqn(4.6)}$$

u(t) is an incoming signal vector, D is a number of the signals which comes to the antenna array, $a(\varphi_i)$ is the steering vectors matrix, S is the source signal vector, n is the noise components in every antenna.

The Incoming signal vector:

$$u(t) = [a(\varphi_1)\ a(\varphi_2)\ a(\varphi_3)\ \dots\ a(\varphi_{D-1})](\ s_0(t)\ \ s_1(t)\ \ \dots\ s_{D-1}(t)\ )^T + n(t) = \boldsymbol{A}s(t) + n(t) \qquad \text{Eqn(4.7)}$$

And s(t) and n(t) are shown in

$$s(t) = (\ s_0(t)\ \ s_1(t)\ \ \dots\ s_{D-1}(t)\ )^T$$
$$n(t) = (\ n_0(t)\ \ n_1(t)\ \ \dots\ n_{M-1}(t)\ )^T$$

By taking the total signal from the antenna array, the input covariance matrix is obtained:

$$\boldsymbol{R_{uu}} = E[\boldsymbol{u(t)u(t+\tau)}]^* = \boldsymbol{AR_{ss}A}^* + {\sigma_n}^2\boldsymbol{I} \qquad \text{Eqn(4.8)}$$

R_{uu} is input covariance matrix, R_{ss} is incoming signal covariance matrix, ${\sigma_n}^2$ variance of the white Gaussian noise. The eigenvalues of the R_{uu} is shown as {λ0,…, λM-1}. This eigen values requires Equation 4.9.

$$|\boldsymbol{R_{uu}} - \lambda_{\boldsymbol{i}}\boldsymbol{I}| = 0; \qquad \text{i=0,1,2,…,M-1} \qquad \text{Eqn(4.9)}$$

If we re-organise equation 4.9 we will find:

$$|\boldsymbol{A}\boldsymbol{R_{ss}}\boldsymbol{A}^* + {\sigma_n}^2\boldsymbol{I} - \lambda_{\boldsymbol{i}}\boldsymbol{I}| = \left|\boldsymbol{A}\boldsymbol{R_{ss}}\boldsymbol{A}^* + ({\sigma_n}^2 - \lambda_{\boldsymbol{i}})\boldsymbol{I}\right| = 0 \qquad \text{Eqn(4.10)}$$

In this case the eigenvalues of $\boldsymbol{A}\boldsymbol{R_{ss}}\boldsymbol{A}^*$ matrix shown as:

$$\mathrm{v_i} = \lambda_{\boldsymbol{i}} - {\sigma_n}^2 \qquad \text{Eqn(4.11)}$$

The matrix A has a full column rank as it is made up of linear independent steering vectors, and Rss signs are not singular unless they are closely related [27]. When the number of incoming signals D smaller than number of elements M, The M-D elements of eigenvalues of $\boldsymbol{A}\boldsymbol{R_{ss}}\boldsymbol{A}^*$ matrix takes zero values. In this case, we will see that according to equation 4.11, $\lambda_{\boldsymbol{i}} = {\sigma_n}^2$ and i=D,D+1,…,M-1. Then we will find.

$$D = M - K \qquad \text{Eqn(4.12)}$$

And qi is a eigenvector which come across to $\lambda_{\boldsymbol{i}}$ eigenvalues:

$$|\boldsymbol{R_{uu}} - \lambda_{\boldsymbol{i}}\boldsymbol{I}|\boldsymbol{q_i} = 0 \qquad \text{Eqn(4.13)}$$

$$\boldsymbol{A}\boldsymbol{R_{ss}}\boldsymbol{A}^*\boldsymbol{q_i} = 0 \qquad \text{Eqn(4.14)}$$

$$\boldsymbol{A}^*\boldsymbol{q_i} = 0 \; ; \qquad \text{i=D,D+1,…,M-1} \qquad \text{Eqn(4.15)}$$

So, the directional vectors corresponding to incoming signal vectors are perpendicular to the eigenvectors of Ruu [18].

$$\{a(\varphi_1)\; a(\varphi_2)\; a(\varphi_3) \ldots\; a(\varphi_{D-1})\} \perp \{q_D, \ldots, q_{M-1}\} \qquad \text{Eqn(4.16)}$$

This is the basics of the MUSIC algorithm. The direction vector of the incoming signal can be estimated by finding the directional vector of the antenna array which is perpendicular to the eigenvectors of Ruu [19].

The eigenvectors of the Ruu covariance matrix belong to either the lower subspaces or the subspaces of noise, from two vertices perpendicular to each other. The steering vectors falling against the DOA are in the sign subspace and thus are perpendicular to the noise subspace. The DOAs (φ_is), which are perpendicular to the noise subspace, can be found by scanning all directional vectors. The matrix of $\mathrm{v_n}$, which contains noise eigenvectors, is generated by scanning noise subspace [27].

$$\mathrm{v_n} = q_D q_{D+1} \cdots q_{M-1} \qquad \text{Eqn(4.17)}$$

As it shown in equation 4.17, the DOA of the incoming signal is:

$$P_{MUSIC} = \frac{a^*(\varphi)a(\varphi)}{a^*(\varphi)v_n v^*{}_n a(\varphi)} \qquad \text{Eqn(4.18)}$$

4.3.2 ESPRIT Algorithm

The development of the MUSIC algorithm is an important success as it takes the multidimensional nature of the optimal solution for estimation of signal parameters in the course of practical approaches [17]. Another method for determining the angle of arrival is the ESPRIT (Estimation of Signal Parameters via Rotational Invariance Techniques) method.

ESPRIT is similar to MUSIC in that it correctly exploits the data model, but offers significant advantages when compared to MUSIC. Unlike other algorithms, ESPRIT does not require detailed information about the antenna array geometry and the nature of each antenna element (e.g. pattern, antenna gain). This also removes the need for storage for multi-dimensional parameter spaces at the same time. ESPRIT is simpler regarding calculation than the other algorithms because it does not apply the scanning process. Also, ESPRIT exhibits improved performance over the conventional MUSIC algorithm regarding deviation and resolution [17].

ESPRIT is based on the determination of the signal subspace and the steering vector generated by the data obtained by two identical antenna sub-arrays. This steering vector can be found by calculating the eigenvalues of the covariance matrix which has the equal size to the amount of the sensor pair. Also, it should be emphasized that all characteristic properties of the array manifold not be needed [17].

The ESPRIT algorithm, which is developed according to the formalisation of the covariance, can be summarised as:

- The correlation matrix Rzz is should be generated by sampling the signals in antennas

- Generalised eigenvalues and eigenvectors of R should be found

$$R_{zz}\bar{E} = I_n\bar{E}\Lambda \qquad \text{Eqn(4.19)}$$

In here the eigenvalue vector Λ and eigenvector matrix is:

$$\Lambda = diag\{\lambda_1, \dots, \lambda_{2M}\}; \qquad \lambda_1 < \cdots < \lambda_{2M} \qquad \text{Eqn(4.20)}$$

$$\bar{E} = e_1, \dots, e_{2M} \qquad \text{Eqn(4.21)}$$

- The number of signal ($\widehat{K}$) should be estimated.
- Separate the eigenvectors $E_x\ and\ E_y$ by determining the signal subspace.

$$E_s = I_n[e_1, \dots, e_{\widehat{K}}] \rightarrow \begin{bmatrix} E_x \\ E_y \end{bmatrix} \qquad \text{Eqn(4.22)}$$

- Find the eigenvalues and eigenvectors of $E_x\ and\ E_y$.

$$E_{XY}{}^H E_{XY} = \begin{bmatrix} E_X{}^H \\ E_Y{}^H \end{bmatrix} [E_X E_Y] = E\Lambda E^H \qquad \text{Eqn(4.23)}$$

And separate the E matrix to submatrixes which have $\widehat{K}x\widehat{K}$ size.

$$E = \begin{bmatrix} E_{11} & E_{12} \\ E_{21} & E_{22} \end{bmatrix} \qquad \text{Eqn(4.24)}$$

- Calculate the eigenvalues of the vector $\Psi = -E_{12}{E_{22}}^{-1}$

$$\widehat{\varphi_k} = \lambda_k(-E_{12}{E_{22}}^{-1}), \qquad \forall k = 1, \dots., \widehat{K} \qquad \text{Eqn(4.25)}$$

- Calculate the DOA by the formulation of:

$$\widehat{\varphi_k} = \cos^{-1}\{c\arg(\widehat{\varphi_k})/(w_0\Delta)\} \qquad \text{Eqn(4.26)}$$

4.4 Conclusion

DOA estimation algorithms can be considered as one of the most critical factors that can increase the cost of the system. For that reason, the main requirements which expected from DOA algorithm should be determined. It is expected that the algorithm used should be set up in such a way that it does not require much memory, and that the capacity needs to be kept at a minimum and not create too much arithmetic load on the processor.

For the project of automatic antenna tracking of a sounding rocket, there is only one target to track. Moreover, because of the fast-moving nature of the target, DOA estimation algorithm should be computationally light and robust. For that reason, technology readiness is also a key factor in choosing the suitable method.

Phase interferometry method is an excellent candidate to satisfy the requirements of our project. However, we should modify that system a bit. Firstly, Automatic Antenna Tracker is not tracking the beacon signal in our mission. Therefore, we should think about how to extract phase data from the received signal which spread by FHSS technique and BPSK modulated. For this reason, the output waveform of payload transmitter should be well known by the receiver.

5 Cross-Correlation Direction of Arrival Estimation Method

Phase interferometer methods depend on the phase differences of the antennas of a DF system, different approaches have been used for measuring the phase difference between the antennas. With the critical advances in the receiver and Analog to Digital Conversion and Digital Downconversion technology, the incident signals received by the antennas are digitised and then processed in the digital world [20].

The FHSS spread and BPSK modulated telemetry signal transmitted through a radio channel. Thanks to, Frequency Hopping Spread Spectrum technique there is lower probability to be detected by an unauthorised surveillance system due to the signal power is lower than the noise floor, and frequency is jumping over the time.

According to operational requirements of Automatic Antenna Tracking System, the tracking station also does not have any prior information about frequency sequence of the FHSS algorithm. This makes difficult to detect and track the signal itself. Furthermore, the received signal includes noise components [28].

However, if the tracking station uses two spatially separated antennas for one dimension with wideband receivers and cross-correlates the two outputs, much of the available processing gain can be accessed, without any a priori knowledge of the signal [29].

The internal receiver noise in different receivers is independent. The antenna noise in the two receivers comes from the same sources, but if these sources can be assumed to be spatially distributed over the full width of the antenna radiation patterns, then the signals from these noise sources arrive at the two antennas with a distribution of time delays. As a result, there is no correlation between the different antenna noise inputs to the different receivers, provided that the antenna separation is large enough. This assumption is critical for automatic antenna tracking application [29].

The proposed system by A.W.Houghton and C.D. Reeve [30] can detect spread-spectrum signals of arbitrary waveform and spectrum, with a power spectral density (PSD) below receiver noise levels, by direct threshold detection applied to the CCF. Forming the cross-spectral density (CSD) by taking the Fourier transform usually produces a frequency-domain signal, which is too noisy. However, the properties of a spread-spectrum signal make it possible to improve the signal to noise ratio (SNR) in the CSD. The signal part of the CCF is the time-shifted Autocorrelation Function (ACF) of the spread-spectrum signal. Owing to the signal's broadband nature, it will be very narrow, is typically a few tens of nanoseconds wide. If the two antennas are separated by only a few metres, then this ACF is shifted from the centre of the total CCF by no more than a few nanoseconds. The noise components of the CCF are spread uniformly over the whole width of the CCF, which will be of the order of milliseconds or more. A time-domain filter

can then be used to select, or window, a narrow central portion of the CCF, capturing virtually all of the signal but rejecting most of the noise. Taking the Fourier transform of this windowed CCF produces the time-domain filtered cross-spectral density (TDFCSD). Threshold detection in this TDFCSD will then not only reveal the presence of a spread-spectrum signal but also give its spectrum [29, 30].

In this chapter, the time domain filtered cross-spectral density (TDFCSD) technique, proposed by A.W.Houghton and C.D. Reeve, will be explained and It will be used as a direction finding the algorithm in Automatic Antenna Tracking System.

5.1 Cross-Correlation Function and Its Properties

The cross-correlation function (CCF) between two complex signals u(t) and v(t) which has finite energy is:

$$r_{12}(\tau) = \int_{-\infty}^{\infty} u(t-\tau)^* v(t) dt \qquad \text{Eqn (5.1)}$$

u^* is complex conjugate of u. The cross correlation is used to find where the two signal will match and what is the degree of similarities of these two signals.

If we assume u(t) and v(t) are the two signals comes from two different antennas. Moreover, u(t) comes earlier than v(t). u(t) arrives at the antenna 1 at t_0 and v(t) arrives to the antenna 2 at $t_0 + \Delta t$. The cross-correlation function between u(t) and v(t) will reach to the maximum value at Δt due to they are only time shifted version of each other. Therefore, it is possible to find TDOA and phase difference between these two antennas. Cross correlation function has some properties.

- Cross-Correlation function exhibits conjugate symmetry:

$$r_{12}(\tau) = r_{12}(-\tau)^* \qquad \text{Eqn (5.2)}$$

- If the cross-correlation of two signals equals to the zero, we say these two signals are orthogonal. Fourier transform property of cross-correlation:

$$r_{12}(\tau) = \int_{-\infty}^{\infty} u(t-\tau)^* v(t) dt = F^{-1}\{F\{u(t)\}.F^*\{v(t)\}\}(\tau) \qquad \text{Eqn (5.3)}$$

Therefore, we can also calculate the cross-correlation of the two signals by using the Fourier Transform of them. F^* denotes complex conjugate of the Fourier transform of the signal.

Discrete cross-correlation also has the same properties.

$$r_{12}[k] = \sum_{i=0}^{N-1} u^*[i-k]v[i] \qquad \text{Eqn (5.4)}$$

As in the continuous case, discrete correlation differs from convolution in that there is no folding operation. Hence, the remaining rules for displacement, multiplication, and summation are performed exactly as for the case of discrete convolution [31].

To compute the discrete cross-correlation:

- Make u(t) and v(t) finite length functions.
- Assume N is the number of samples which defines u[k] and v[k]. It is computationally easier if we choose $N = 2^a$ when a is an integer.
- Apply the zero-padding to u[k] and v[k].
- Take FFT of the zero-padded u[k] and v[k] signals.
- Take the complex conjugate of U[n] by changing the sign of the imaginary part
- Calculate the inverse FFT of $U^*[n]V[n]$.
- Moreover, the result is the discrete cross-correlation function $r_{12}[k]$

Then, we can estimate TDOA by finding the position of the κ with $\Delta t = \kappa/f_s$, and Δt is the place where the cross-correlation function is the maximum [28].

ZERO PADDING

Zero padding is a crucial operation we should apply before applying FFT to the signals. Zero padding allows one to use a longer FFT, which will produce a longer FFT result vector. A longer FFT result has more frequency bins that are more closely spaced in frequency. However, they will be essentially providing the same result as a high quality "Sinc" interpolation of a shorter non-zero-padded FFT of the original data.

This might result in a smoother looking spectrum when plotted without further interpolation. Although this interpolation will not help with resolving or the resolution of and between adjacent or nearby frequencies, it might make it easier to visually resolve the peak of a single isolated frequency that does not have any significant adjacent signals or noise in the spectrum. Statistically, the higher density of FFT result bins will probably make it more likely that the peak magnitude bin is closer to the frequency of a randomly isolated input frequency sinusoid, and without further interpolation (parabolic et al.). However, essentially, zero padding before a FFT is a computationally efficient method of interpolating a large number of points [32].

Zero-padding for cross-correlation is used not to mix convolution results (due to circular convolution). The full result of a linear convolution is longer than either of the two input vectors. If a place is not provided to put the end of this longer convolution result, FFT fast

convolution will just mix it in with and cruft up the desired result. Zero-padding provides a bunch zeros into which to mix the longer result. And it is much easier to un-mix something that has only been mixed/summed with a vector of zeros.

In the case of zero-padding, the signal in the time domain and also applying the window function, windowing the signal should be before zero-padding. If the window function applied after the zero-padding, the result would still have a sharp transition from the signal to zero instead of a smooth transition to zero [31].

5.2 Cross Spectral Density

Cross-Spectral Density (CSD) denotes the Fourier transform of the cross-correlation function.

$$R_{12}(f) = F\{r_{12}(\tau)\} = F\{v(t)\}.F^{*}\{u(t)\} = U^{*}(f)V(f) \qquad \text{Eqn(5.5)}$$

However, in practice, CSD is the FFT of the $\{r_{12}[k]\}$. According to Fourier's theory, the time shift in the time domain means a phase slope in the frequency domain. Assume that, there is no noise. Then:

$$U(f) = e^{-j2\pi f \Delta t}V(f) \qquad \text{Eqn (5.6)}$$

Δt denotes time difference between channels, estimating the unknown Δt in the time domain by maximization of the magnitude of the CCF has been transformed into fitting a straight line to the argument of the CSD. In Figure 5.1, the linear portion of the phase is used to estimate Δt [6]. The slope of the linear part in Phase diagram of the CSD will give the Δt.

Moreover, also, the phase of the $R_{12}(f)$ (in Equation 5.5) is the phase difference between U(f) and V(f) for all frequencies due to the multiplication of one complex signal with complex conjugate of another signal. Then, the knowledge of the phase difference between the channels will give the DOA according to the equation 4.2 [28].

We have already mentioned three different cross-correlation direction finding methods in chapter five. These are;

- Finding the maximum point in cross-correlation function and estimating TDOA according to its place.
- Calculating the cross-spectral density and calculating the phase slope of the linear part of the phase diagram.
- Estimation of the phase difference and the frequency bin in the CSD.

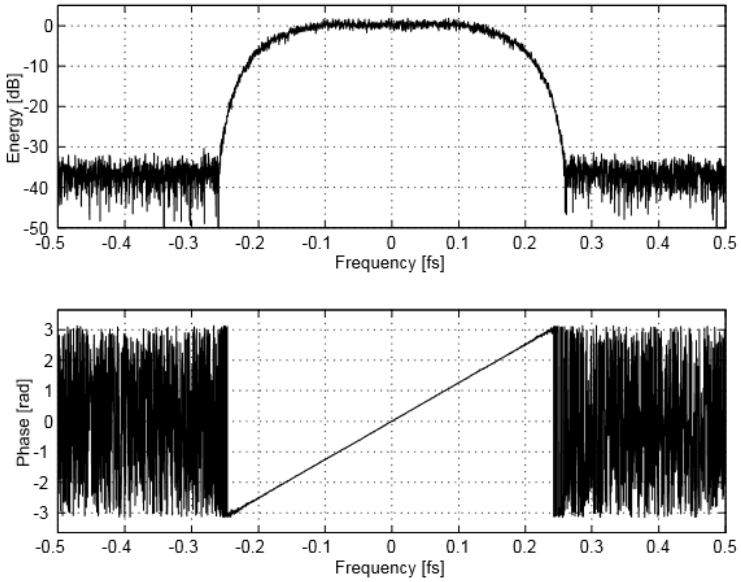

Figure 5.1: Typical Energy and Phase Representation of the CSD [32]

5.3 Cross-Correlation Direction Finding Antenna Tracker

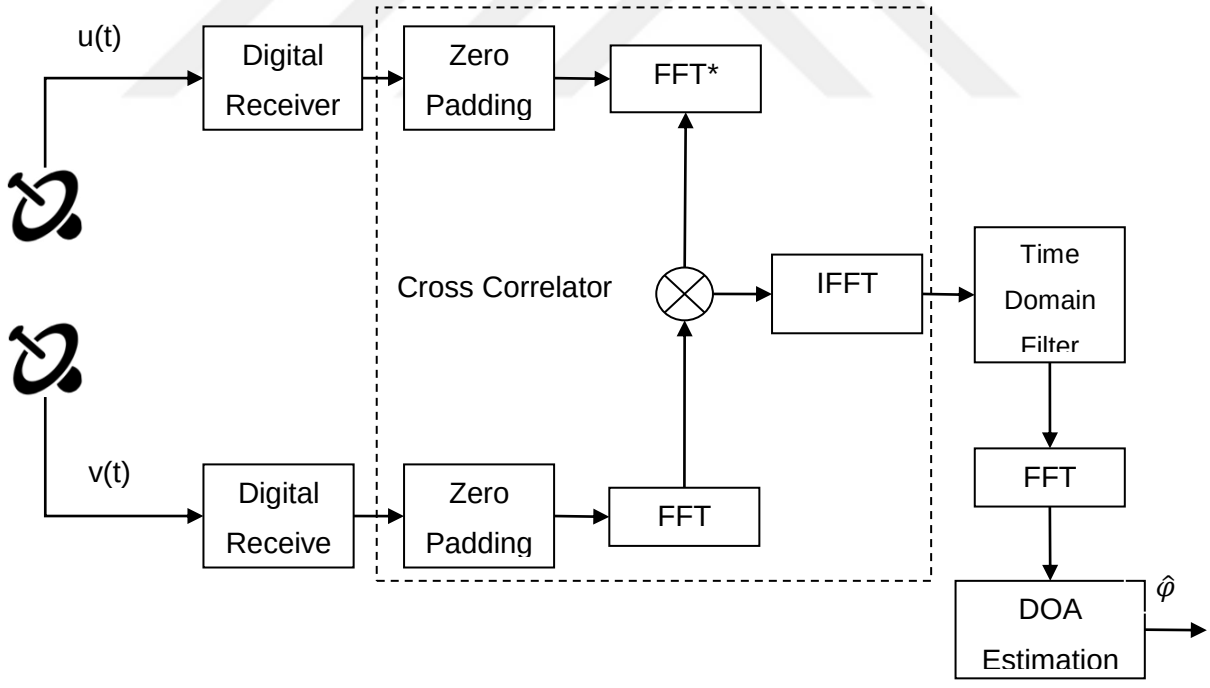

Figure 5.2: Block Diagram of The Proposed DF System for 1-D Tracking [28]

Two antennas and receivers require to track the target in 1-Dimension in the case of there is no phase ambiguity. In the case of tracking the target in azimuth and elevation

dimensions, we need four antennas. As it is mentioned in the fourth chapter, if the system has antenna separation distance longer than the half of the minimum wavelength, the phase ambiguity will occur. For solving this problem, third antenna needed for every dimension. Our system is working on ISM 2.4 GHz band. Therefore the wavelength is too short to choose antenna separation distance shorter than the half of the wavelength. By using the one antenna common for both dimensions, to solve phase ambiguity, minimum five antennas required for automatic antenna tracker

6 Simulation Methodology

The primary goal of the work is determining the design parameters of Automatic Antenna Tracking system to make possible to implement it. The main approach to study is simulating the Rocket Tracking case in MATLAB and Simulink tools cooperatively. The modular approach is applied while simulating the real world application in the tools. The system modelling has been done by Simulink, and every sub-system is designed and programmed in MATLAB simulation tool. This modular approach gives freedom to the programmer to design every subsystem independently, and easiness of diagnosing the fault. In the case of a fault occurred, our approach is flexible to solve the problem without changing any parameter in other subsystems.

6.1 Definition of the Problem and Designing the Conceptual Model

As it is explained in chapter one, an automatic antenna tracking concept must be realised to support the reception of the payload data during launch and descent phases. All the telemetry shall be received by more than one ground stations along the launcher and payload descending trajectory for redundancy. Receiving telemetry and tracking the signals should be done by observing stations. To ensure communication quality, during launch and descent phases, automatic antenna tracker should track the telemetry signal. We can summarise our goal in two groups.

- Telemetry Signal Generation
- DOA estimation of the sounding rocket

6.1.1 Telemetry Signal Generation

The signal generator models two things, moving of the target and hardware of our system.

6.1.1.1 Target Model

According to flight data required by the team, the maximum expected the angular rate of the LAPAN sounding rocket is shown in Figure 6.1 and Figure 6.2. This shows that the direction finding algorithm should be computationally light and also this determines the mechanical requirements for antenna controller. In this project, we will not design the antenna controller. The automatic antenna tracking system will find the DOA of the telemetry signal according to antenna array's body axis. This denotes the angle difference information for the antenna controller.

Nevertheless, the relative speed of the sounding rocket is also critical information due to doppler shift phenomena in telemetry signal. Because the telemetry system uses wideband spread spectrum communication technique, the doppler shift is not affecting the

system performance. Automatic Antenna Tracker receiver is a wideband digital receiver, and the DOA information is independent of the frequency itself due to the tracker is using cross-correlation DF method.

These figures are generated by Indonesian team members of the project as an input of automatic antenna tracker.

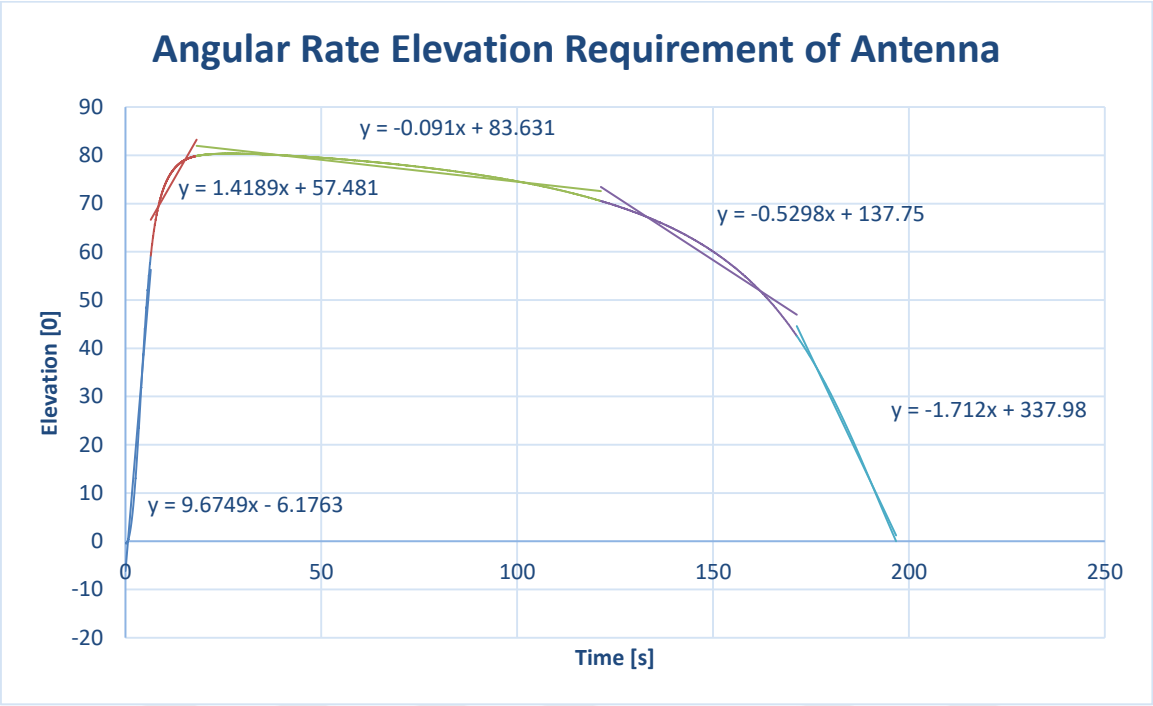

Figure 6.1: Angular Rate Elevation Requirement of Antenna

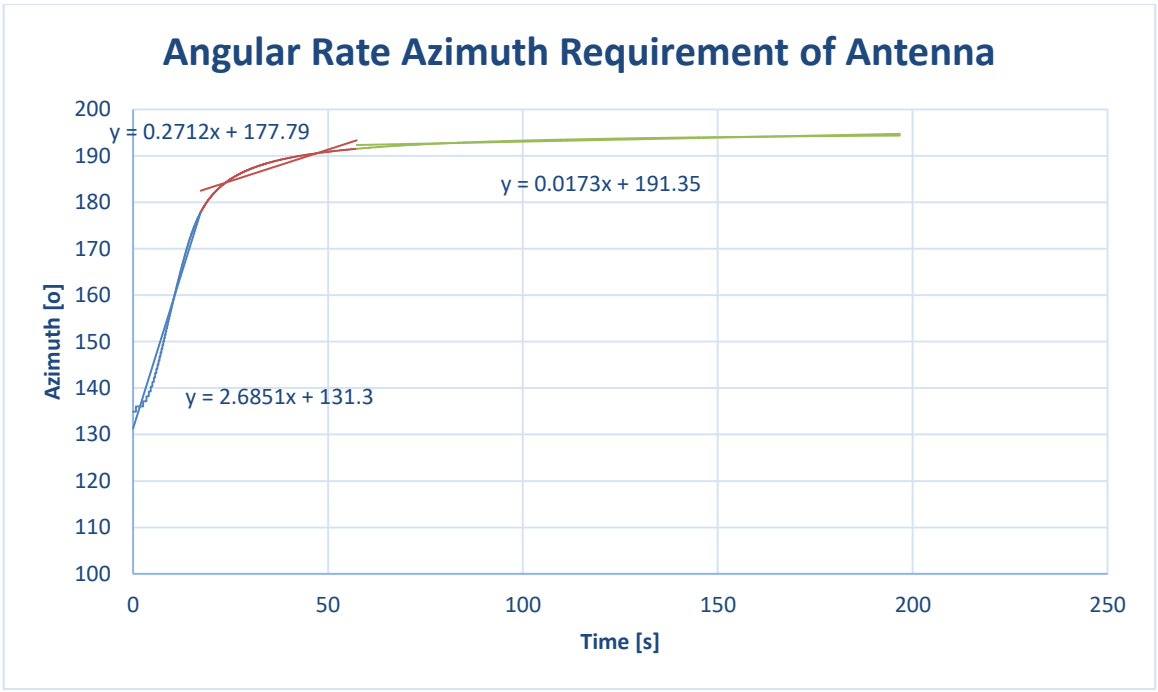

Figure 6.2: Angular Rate Azimuth Requirement of Antenna

6.1.1.2 Hardware Definition

The antenna array elements are helical antennas which have 18dBi gain, and the full beam-width is 27°Full Wave Half Maximum, this means even in 13.5° error the tracking function can be operated. However, the Field of View (FOV) of the primary communication dish is 6°. Therefore, maximum error angle requirement for antenna tracker is determined as 3°.

The telemetry signal is BPSK modulated in ISM 2.4GHz band (2400 MHz-to-2483,5 MHz) and the data stream in 50000 bps. However, the transmitter is using FHSS technique and frequency is jumping around 20 MHz. Therefore, the receiver should have minimum 20 MHz bandwidth.

Digital Receiver Model

Many digital receiver technologies have been analysed during the research of received signal waveform. There are some constraints for choosing the right receiver concept for antenna tracker:

- The cost of the receiver technology is a fundamental constraint
- Technology readiness, availability of required peripheral devices.

  For instance, direct sampling ADCs and receiver design concept is a cutting-edge technology for wideband high-frequency receivers. Direct sampling means there is no down converter, or any mixer, or filter circuit in the receiver. Conventional analogue-to-digital converters (ADCs) are fundamentally limited by timing jitter in the sampling source, forcing a trade-off between bandwidth and resolution. As a result, radio frequency (RF) systems are typically designed with narrow-bandwidth channels. These engineering constraints present problems when faced with broadband signals and ultra-short pulses. At high carrier frequencies, RF systems are further limited by the tuner that must mix down to baseband for electronic digitisation.

  However, this system requires a massive amount of memory. Antenna tracking receiver working in high frequency and also has four channels direct sampling of this signals lead us sampling under Nyquist Frequency and this increased complexity and the cost of the receiver. Furthermore, this makes direction finding algorithm computationally dense and small. Therefore, this design approach is not appropriate for tracking fast moving targets like a sounding rocket.

As it is mentioned in [1, 2, 4], One of the most suitable receiver technique for FHSS DF is acousto-optic cross-correlation receiver. According to literature, it is possible to construct acousto-optic correlator until 1 GHz bandwidth; a large detection bandwidth is obtained. Furthermore, the acousto-optic correlator enables real-time DOA estimation [28, 29, 30].

We assumed that the cross-correlator is digital in our simulation. The down converter reduces the frequency to the IF levels and ADC digitise this analogue signal after.

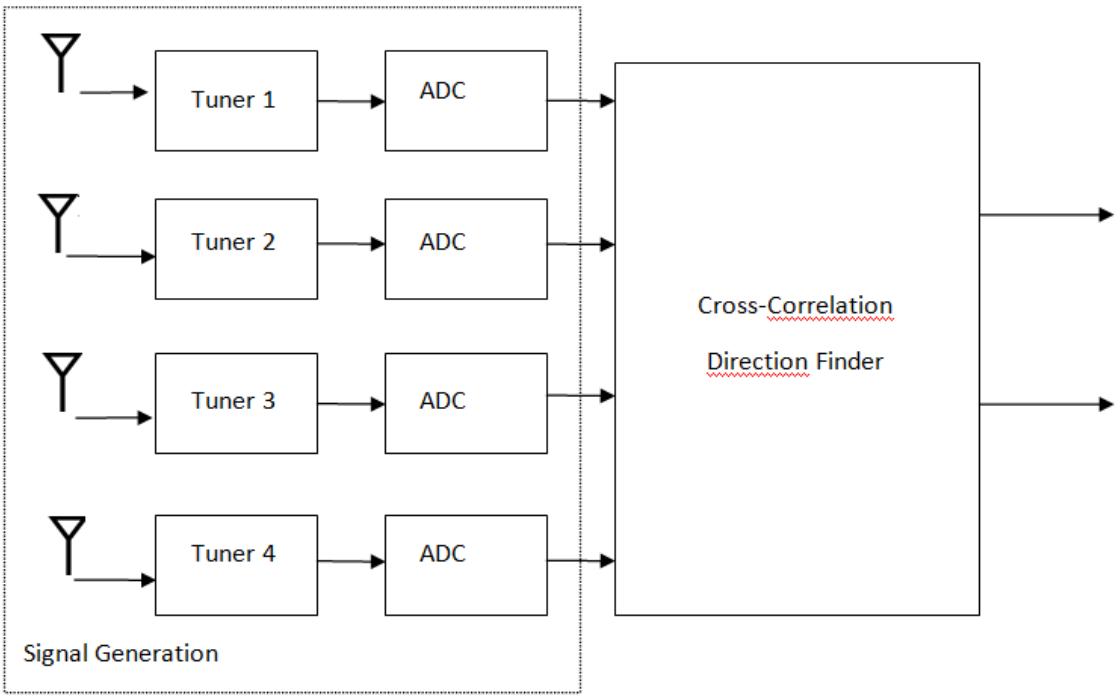

Figure 6.3: Block Diagram of Simulation Methodology

6.1.2 DOA Estimation of the Sounding Rocket

As it is described in chapter four and chapter five, cross-correlation interferometer method is appropriate to approach for using in Automatic Antenna Tracker. Due to the massive dimensions of the Simulink system design, the direction finding Simulink diagram is not possible to print on this dissertation. However, the reader can find the files in dissertation DVD. Every block of the Tracker will be explained in this part of the dissertation.

6.1.2.1 Antenna Array Models

The antenna array which has designed for antenna tracker is shown in Figure 1.4 and Figure 6.4. Two spatially separated antennas are enough to track the target in 1-Dimension in the case of the antenna separation distance is smaller than the half of the wavelength. However, because of the three reasons, it is not possible for tracking sounding rocket in ISM 2.4 GHz band.

- The wavelength is too short for placing antennas in that distance. The wavelength of the system is around 6 cm, and half of it is around 3 cm while the diameter of the highly directive antenna is larger than 5 cm.

- According to the results of the MATLAB and Simulink simulations, the accuracy of the antenna tracking system will increase by distance. The literature also supports this result [28, 29, 20, 30]

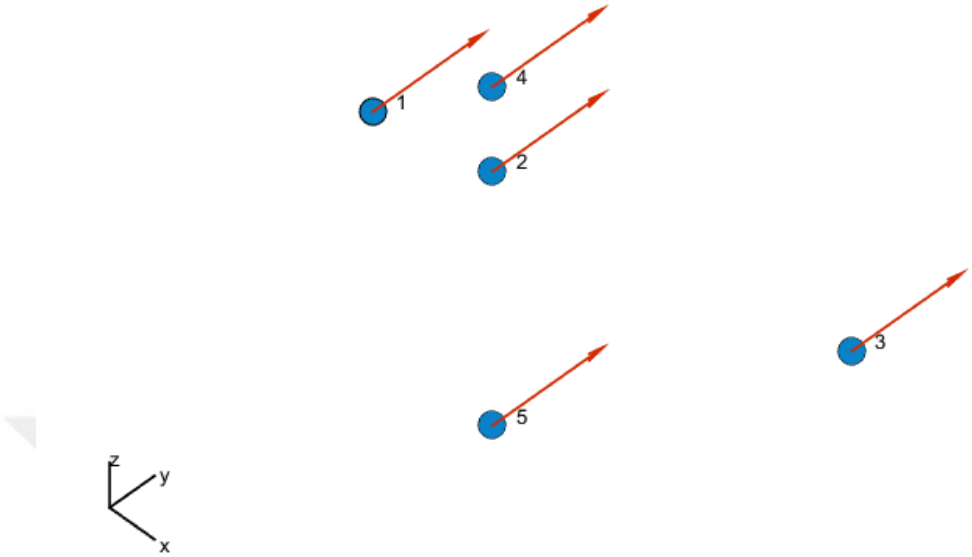

Figure 6.4: 2-D Antenna Array Configurations for Tracking Receiver

- The mutual coupling between antennas will be too high in short distances due to antenna elements have high directivity and gain, and antenna noise will be correlative with each other. Even though the correlative interferometer concept is robust method to un-correlative noises, the correlative noise can be fatal for tracking system

Because of that reasons, antenna separation distance has been chosen a few orders of the wavelength. However, the phase ambiguity problem will occur when we choose the separation high. Long Base Interferometry approach recommended for the automatic antenna tracking system. In that approach, the third antenna is used for every dimension. The planar antenna array is assumed as two different sub-arrays (two different linear arrays). Every tracking dimension is tracked by one linear antenna array, and one antenna is used commonly for every linear array. By this way tracking the sounding rocket in azimuth and elevation dimensions is possible with five antenna elements instead of six.
Increasing of antenna separation distance will make the solution lines closer to each other, as it is described in Figure 4.9, this effect increase the possibility of errors in DOA estimation. In this study, the antenna separation distance is optimised carefully for automatic antenna sounding rocket tracker.

6.1.2.2 Signal Generator Model

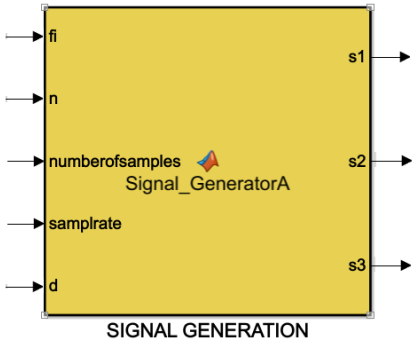

Figure 6.5: Signal Generator Model

Signal generator Model represents all the processes before the cross-correlation direction finder in the simulation. The main responsibility of it is producing S1, S2 and S3 antenna signals with respect to inputs. The inputs of this model are real DOA value (fi), number of multiple computations (n), number of samples in the received signal, the sampling rate, and the distance between antennas.

In this system model,

- The parameters which are used in the function has been defined. These are :
  - Carrier frequency, Frequency hopping rate, message rate, frequency hopping time offset.
- Message generation and frequency hopping ignition generation have been done.
- Time domain definition for sampling the signals we have generated has been done.
- Modulation of the signals and Generation of the signals on Antenna Elements without noise has been done.

The MATLAB software has been used while simulating every subsystem. Frequency hopped spread spectrum signal is shown in Figure 6.7.

6.1.2.3 Channel Model

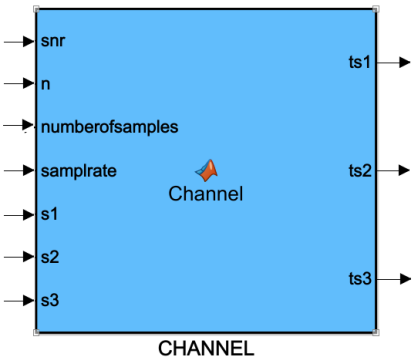

Figure 6.6: Channel Model

The communication channel assumed AWGN (Additive White Gaussian Noise) channel. It means, the channel is adding white noise, which has zero variance and average, on telemetry signal. The noise which wireless channel generated is assumed as un-correlative. This subsystem is modelling this behaviour of the channel in the simulation.

In this system model:

- Independent noises created for every radio channel and it is added on s1, s2, and s3 signals.
- The outputs of the subsystems are ts1, ts2, and ts3

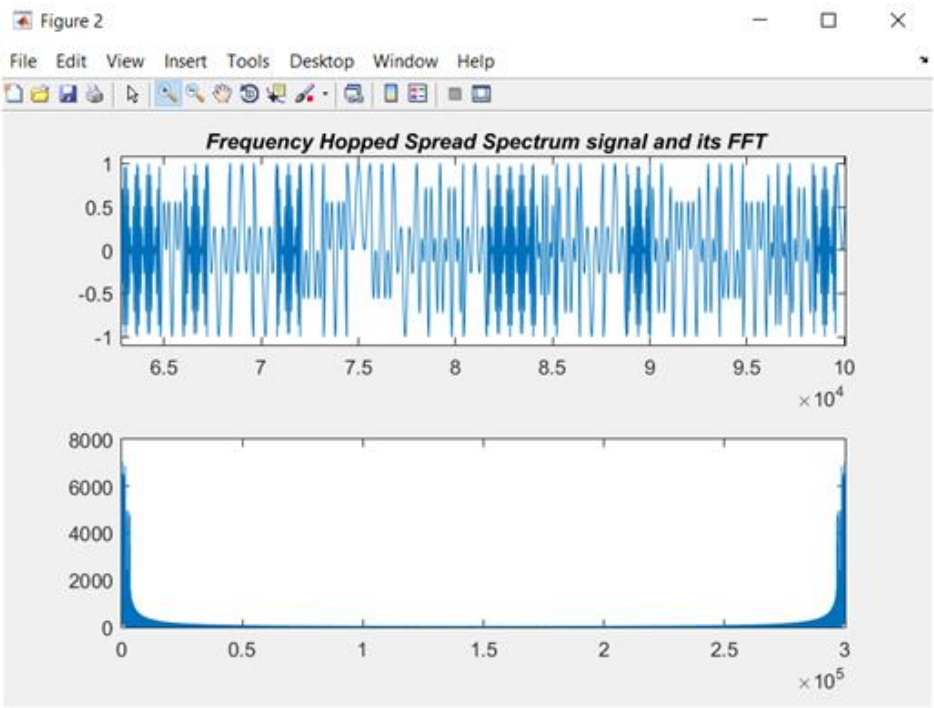

Figure 6.7: Frequency Hopped Spread Spectrum Signal and Its FFT

6.1.2.4 Cross Spectral Functions Model

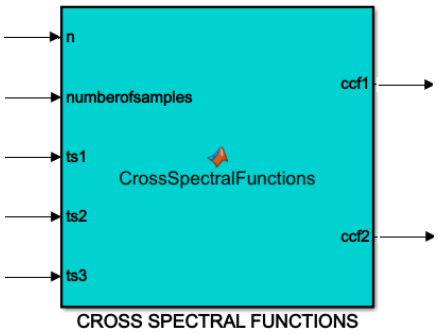

Figure 6.8: Cross Spectral Functions Model

The main goal of this model is generation cross-spectral density (CSD) function and cross-correlation function(CCF). This model is using a number of samples, ts1, ts2, ts3 as an input and generating CSD and CCF functions for short and long base interferometers.
In this model:

- ts1, ts2 and ts3 signals are first zero padded.
- Then FFT is applied to this signals.
- CSD is generated for long base and short base antennas by $CSD = fft(ts1).fft^*(ts2)$ $CSD = fft(ts1).fft^*(ts3)$
- CCF is generated by inverse FFT of CSD.
- ccf1 and ccf2 are outputs of the subsystem.

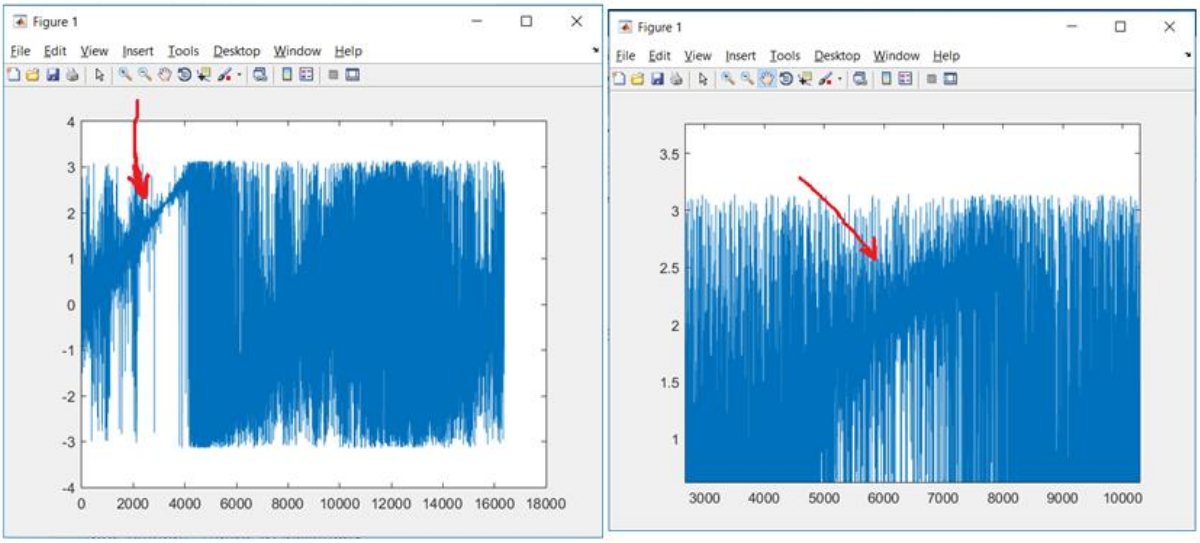

Figure 6.9: Phase Spectrum of Cross Spectral Density Function a) without Gaussian Noise b) with Gaussian Noise

Figure 6.9 shows the CSD function with and without Gaussian Noise. The slope in the linear part of CSD is the $2\pi\Delta t$ which we are searching for. The effect of noise on the CSD also can be seen in Figure 6.9. A phase slope estimation, by applying the least squares, will then give the TDOA for the signal. This method has been used in the references [28, 29, 30]. In Figure 6.8, the SNR (Signal-to-Noise Ratio) of the system is 10dB, DOA is 45°, number of samples of the received signal is 16384 (2^{14}), sampling rate is 300 MHz, and the antenna separation distance is 12 cm (2λ). The amplitude spectrum of cross spectral density under the same conditions is:

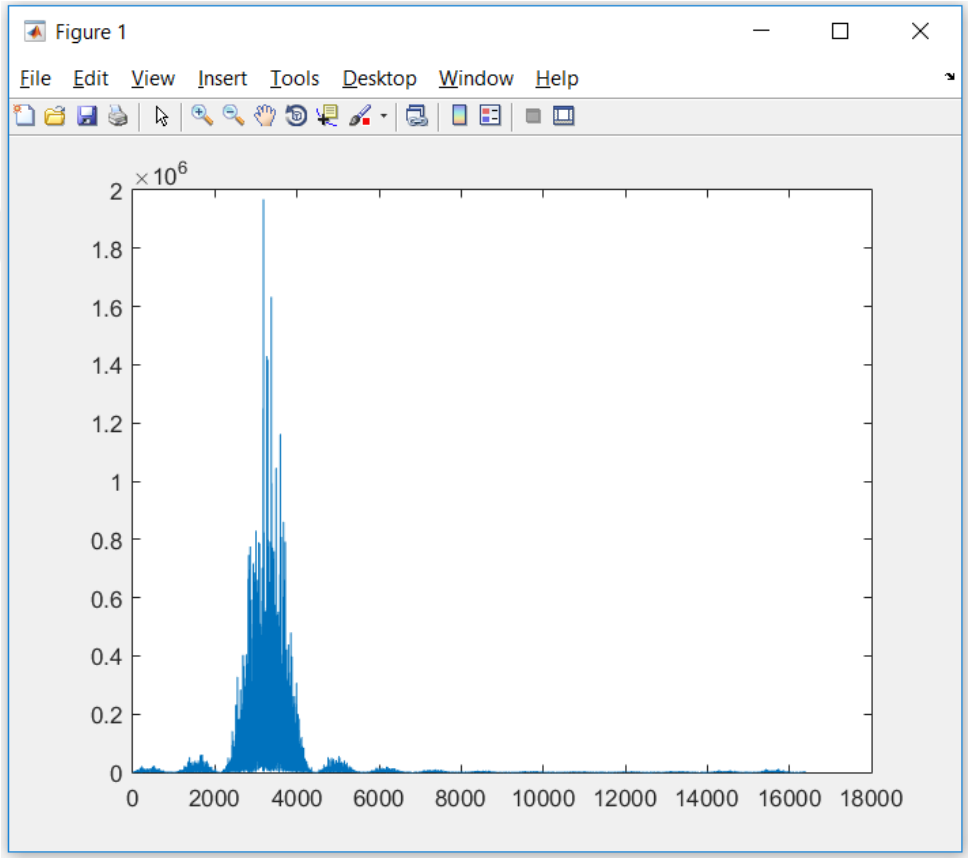

Figure 6.10: Amplitude Spectrum of Cross Spectral Density Function

In the proposed automatic antenna tracking system, Estimation of the phase difference and the frequency bin in the CSD method has been used. The frequency of the bin with the highest magnitude in the CSD is chosen, and the phase difference between the channels is obtained by the phase of the CSD for this bin. DOA can be estimated by knowing this. The phase difference estimation becomes much stable due to the choosing of the frequency bin which has the highest SNR [28].

The phase slope estimation method has not got the advantage of choosing the highest SNR frequency bin. Therefore, it does not show satisfactory performance for antenna tracking system. A method taking the average of antenna bearing angles (DOAs) can be

useful. However, applying this such a method will take time more. Therefore, it is not appropriate for the fast-moving targets like sounding rockets.

6.1.2.5 Time Domain Filtering Model

Time Domain Filtering Model is applying Gaussian windowing on cross-correlation function. When the received signal includes noise, the two sets of independent noise will be spread in cross spectral density. In the case of there is bursty noises like sun explosion on the frequency of telemetry FHSS signal, our data will be under the noise floor, and it will be impossible to localise the signal. The highest frequency bin would be generated by noise or any interference in ISM 2.4 GHz band. In the case of knowing the table of frequencies which FHSS system, fast frequency hopping system would be recommended. However, tracking the telemetry signal which changes the frequency fast is much more difficult than slow change FHSS system.

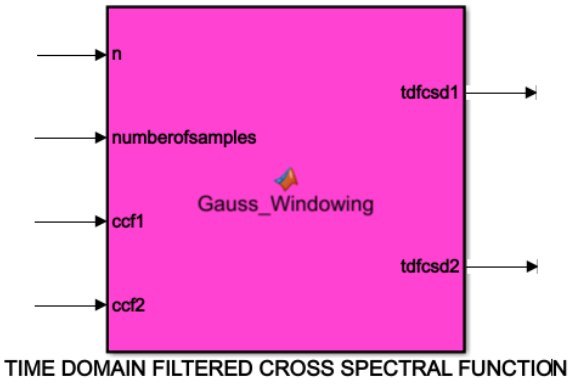

Figure 6.11: Time Domain Filtering Model

Windowing the narrow central section of the cross-correlation function will include most of the FHSS/BPSK signal while rejecting most of the noise. For that reason, the idea of windowing has critical importance for the automatic antenna tracking system. The result of the windowed cross-correlation function is Time Domain Filtered Cross-Correlation Function (TDFCCF), and Fourier transform of TDFCCF is the Time Domain Filtered Cross Spectral Density (TDFCSD) which is the output of Time Domain Filtering subsystem.

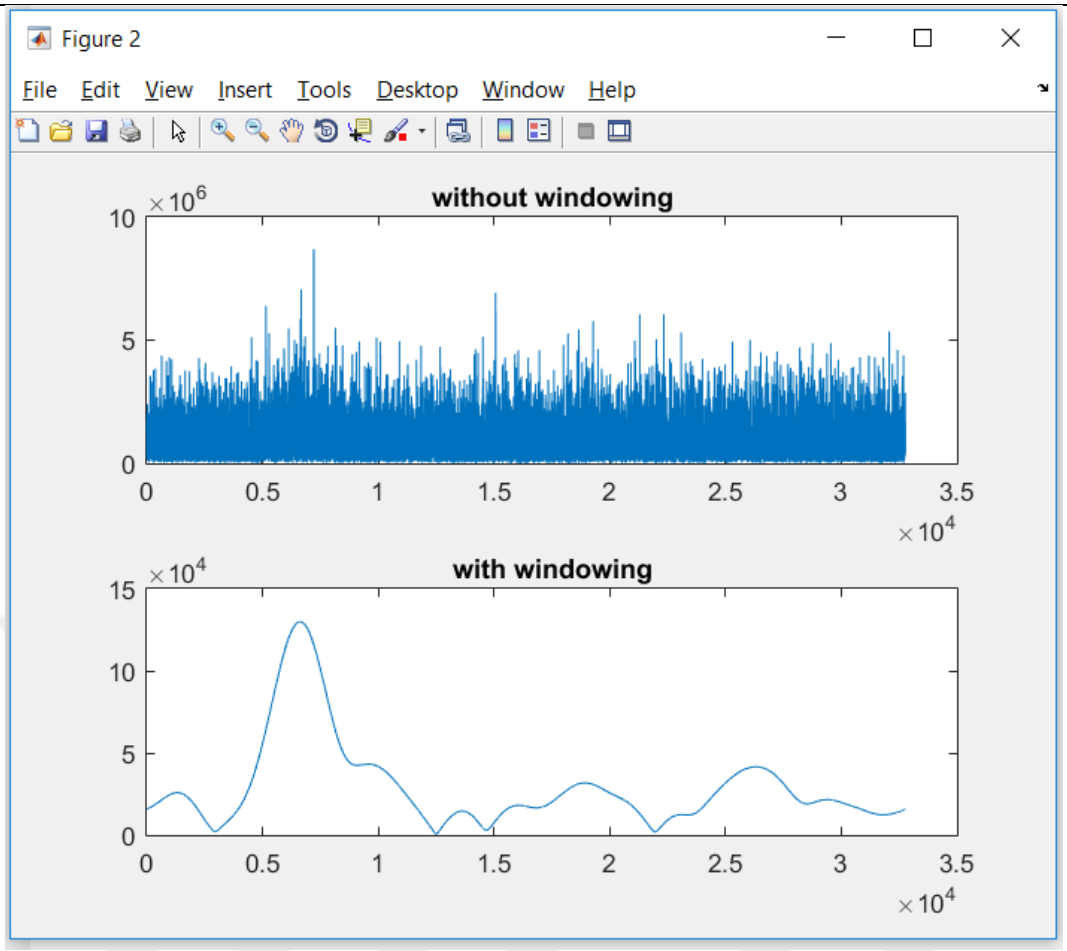

Figure 6.12: CSD Function a) without b) with Gaussian windowing (TDFCSD)

Figure 6.12a shows cross-spectral density function when the Intermediate frequency (IF) is 60 MHz, which is the frequency the downconverter of the receiver reduced the ISM 2.4GHz to, SNR is -10 dB, sampling rate is 300 MHz, the number of samples of the received signal is 16384, incoming DOA is 45 degrees, and the antenna separation distance is 12 cm (2λ).

WINDOW FUNCTIONS

Window functions (or shortly windows) are structures being used to eliminate undesired oscillations in FIR (Finite Impulse Response) digital filter design. Window function has parameters, which affect window performance, such as main lobe width, ripple ratio and sidelobe roll-off ratio. The main aim of window function design is to reach amplitude spectrum providing desired properties with low degree and optimum spectral parameter values [33].

If the length of the window is $1/10^{th}$ of the cross-correlation function, the spectral resolution in cross-spectral density will be reduced ten times. In the case of tracking the broadband signals, it is acceptable. The critical point for designing the window function is

securing the phase of a component of TDFCSD. In the case of the phase component is distorted by a window function, estimation of DOA becomes impossible.

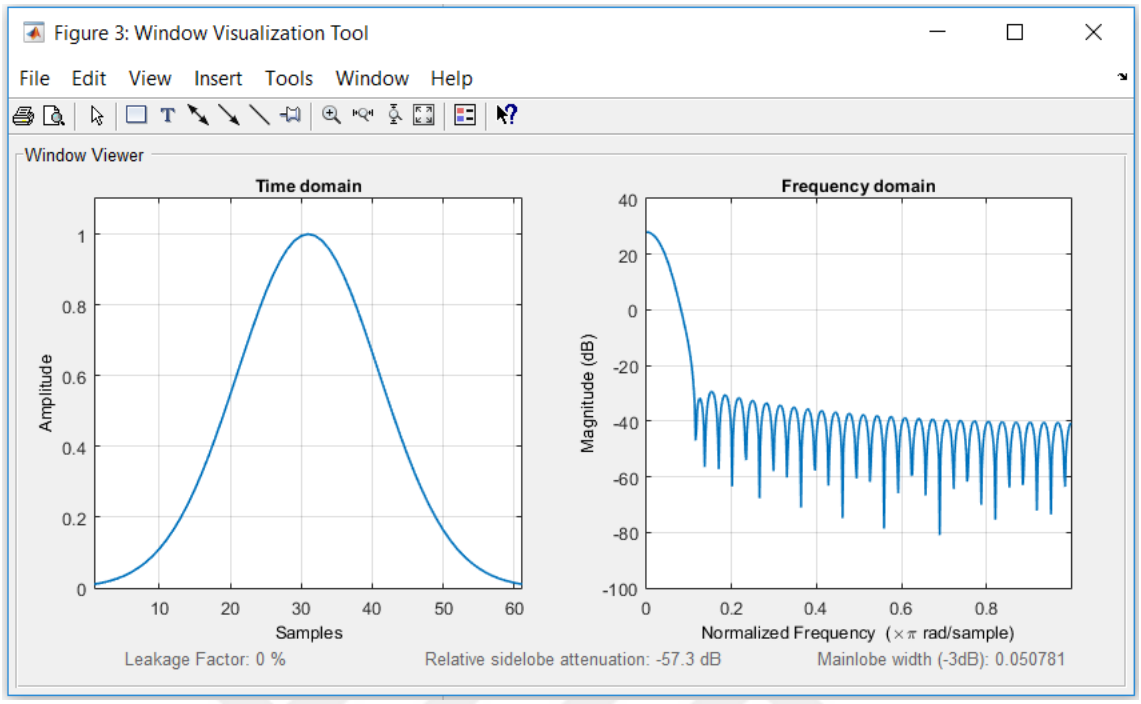

Figure 6.13: Gaussian Window with the length(N) 60

In Figure 6.13 and 6.14, Gaussian window and the effect of the length can be seen clearly. Using wider window in time domain denotes narrower main lobe in the frequency domain. Therefore, it causes narrower region with a linear part of phase which in the middle of the phase spectrum [28]. Choosing and designing window for cross-correlation direction finder, which is used in automatic antenna tracker, is not easy due to the securing CSD from phase distortion. In this research “wintool” and “window visualisation tool” has been used to design and choose the correct window function.

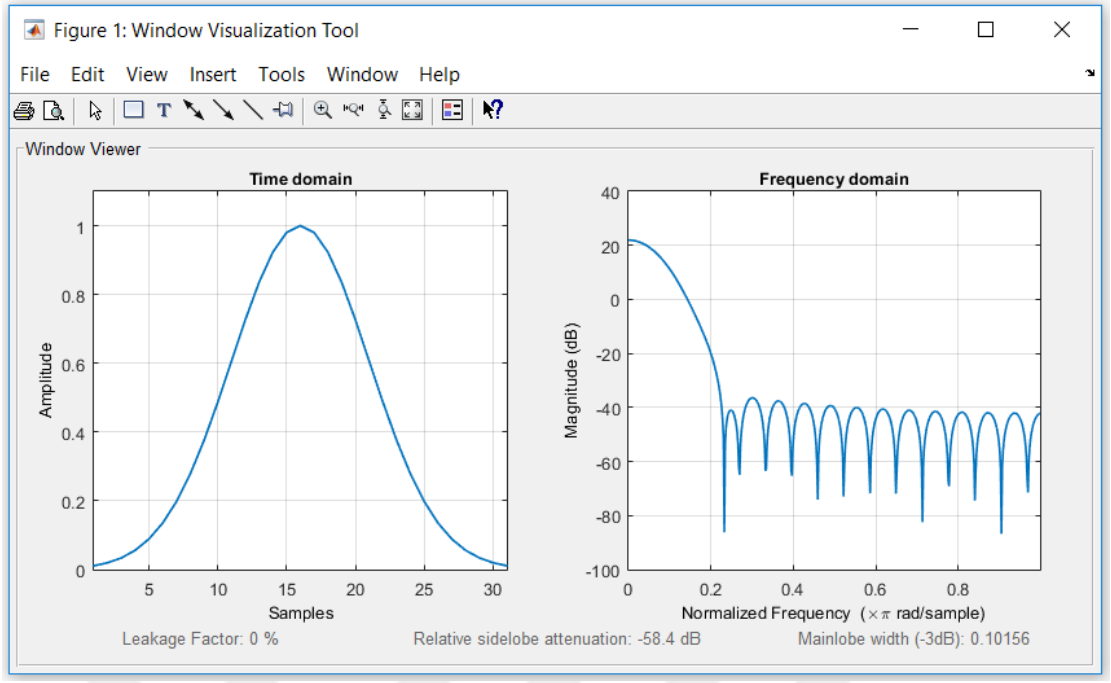

Figure 6.14: Gaussian Window with the length(N) 30

We have analysed Rectangular, Gaussian, Hamming, Triangular and Hanning window functions while choosing due to they recommended by literature [28].

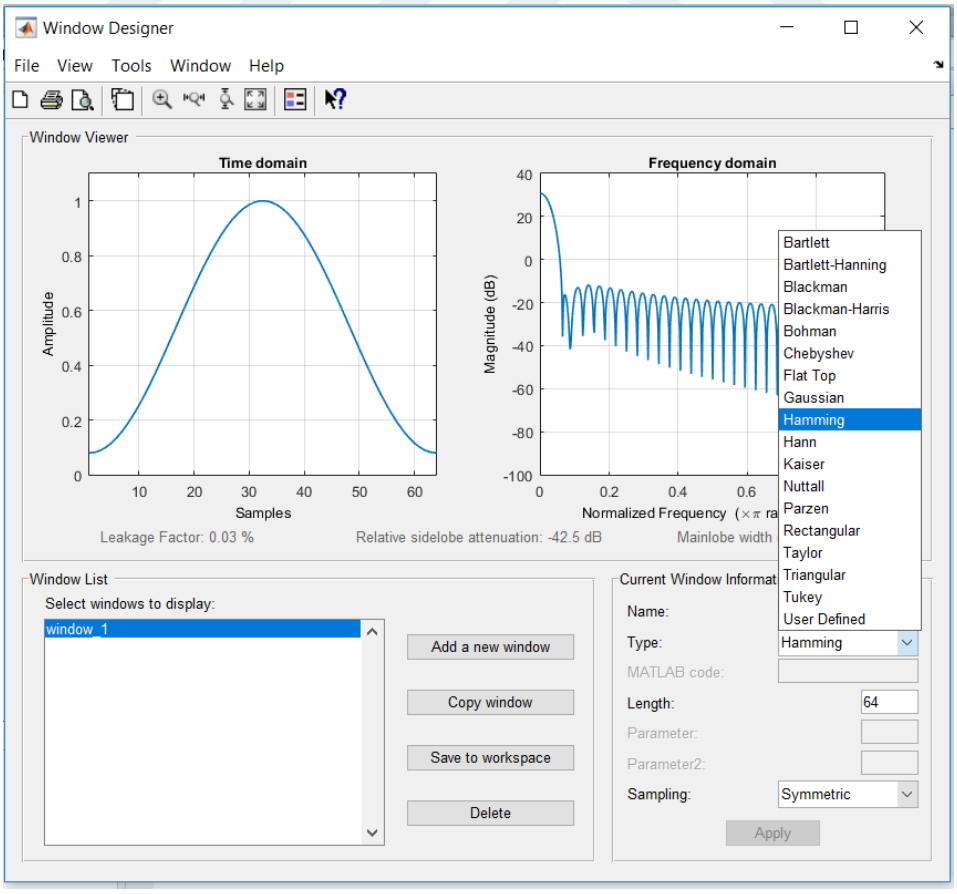

Figure 6.15: Window Designer Tool in MATLAB 2017 and Window Function Options.

Also for FHSS signal, it is observed that Gaussian, Hamming and Hanning windows are working better than Rectangular and Triangular window functions. The Gaussian window function has been chosen due to its availability in phase spectra for linear phase part. w[n] is the Gaussian filter function which has applied. Especially, α=3 and N=30, window length, has been chosen for cross corelarelation interferometer to generate TDFCSD.

$$w[n] = \exp[(-1/2)[\alpha \frac{n}{N/2}]^2], \qquad 0 < |n| < \frac{N-1}{2} \qquad \text{Eqn(6.1)}$$

6.1.2.6 DOA Estimation and Phase Ambiguity Solution Model

In this subsystem, an implementation of the FHSS Signal Elevation and Azimuth DOA Estimation and the solution of the phase ambiguity problem has been done.

- Phase in phase spectrum of the TDFCSD is founded
- The maximum component of the Cross Spectral Density has been detected.
- Phase Ambiguity has been solved for azimuth and elevation angles with the help of the third antenna which has been used in every dimension.
- Finally, azimuth and elevation angles have been estimated, and error of our DOA estimation has been calculated for every millisecond.
- These data have been shown in Simulink also.

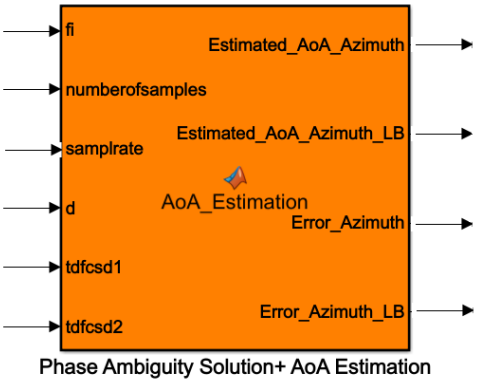

Figure 6.16: Phase Ambiguity and DOA Estimation Model

The phase difference calculated by the phase calculation component is always between -π and π. The true phase difference is not limited to this range. The true phase difference between the antennas is Δφ + I2π where Δφ is the measured phase difference, and I is an integer corresponding to the number of full 2π phase changes. In order to accurately calculate the phase difference the algorithm needs to determine the appropriate value for I. By calculating the phase differences between antenna 1 and 2 and antenna 1 and 3, the algorithm is able to find the number of full phase changes that occur between the

antennas. The maximum number of full phase changes is limited by the wavelength of the signal, the antenna separation, and the field of view. As it is described in chapter four and the literature [6], the technique which used for solving phase ambiguity has already been explained in the section 4.2.2.2 in detail. The MATLAB model included a function that calculated the optimal antenna separation for the first and third antennas given the separation between the first and second antenna and the maximum frequency.

6.2 Computer Simulation Results

The summary of the simulation conditions are

- There is no any interrupt on FHSS/BPSK signal
- The wireless channel is Additive White Gaussian Noise channel
- There is no Interference signal

And the parameters which have been used used;

- The sampling rate is 300 MHz
- The Intermediate Frequency is 60 MHz
- True DOA is 45 degrees
- Distance between antenna 1 and antenna 3 (Long Base) is 2λ (12 cm) for short base 6 cm (λ)

6.2.1 Antenna Separation Distance Versus Estimating Error

The antenna separation is the only parameter we have physical control over and, by extension, have the ability to optimise. As it is described in chapter four, the ideal antenna separation maximises the spacing of phase ambiguity lines and reduces the probability of error. The MATLAB model calculates the optimal separation between antennas 1 and three based on the maximum expected carrier frequency and the separation between antennas 1 and 2. Higher carrier frequencies result in more ambiguities, so estimating a 2.4 GHz ISM band telemetry signal with no ambiguities is an ambitious goal. The minimum separation between antennas 1 and 2 is 6 cm because the antennas themselves are 5 cm wide. To determine the optimal antenna spacing between antennas 1 and 2, we tested all antenna 1-2 spacings between 6 cm and 20 cm with a step size of 0.5 lambdas. The optimal position of antenna 3 was calculated using our spacing function. For taking the average of the estimation error, the azimuth and elevation angle calculated 50 times.

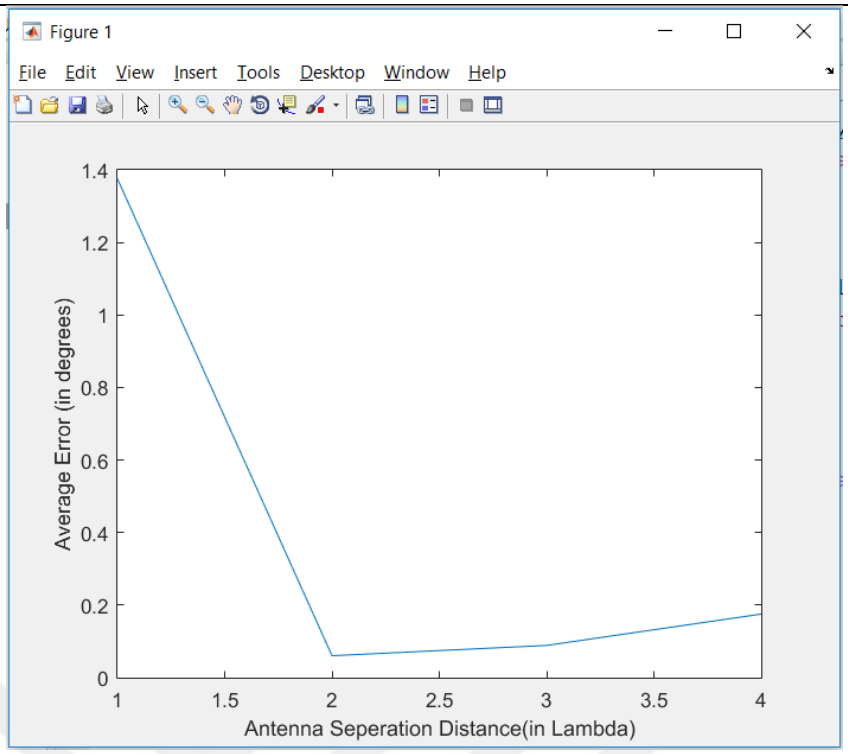

Figure 6.17: Antenna Separation Distance Versus Average Estimation Error

As it is seen from the calculations, the best distance choice is 2λ for automatic antenna tracker's cross-correlation direction finder.

6.2.2 Signal-to-Noise Ratio(SNR) Versus Estimating Error

Increasing SNR naturally increase the estimation accuracy of the direction finder. According to Link Budget of the telemetry system is like below:

- Transmitted Power: 30 dBm
- Tx Antenna Gain: -10 dBm
- Tx Line Loss: 0.5 dBm
- Free Path Loss: -138.92 dB
- Rx Antenna Gain: 18 dBi
- Rx LNA Gain: 14 dB
- Polarisation Loss: 3 dB
- Total Estimated Signal Power : -90,92 dBm

Therefore, the receiver sensitivity should be around -97 dBm. The digital receiver will take the signal, and for the IF (Intermediate Frequency) signal SNR levels will be around 10 dB s due to the Receiver gain.

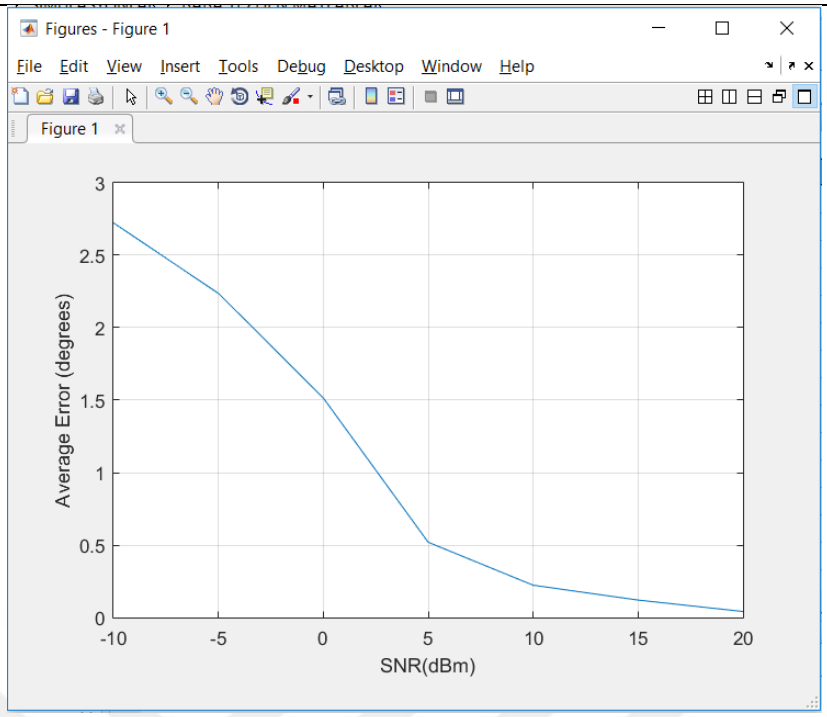

Figure 6.18: Signal-to-Noise Ratio Versus Average Estimation Error

While plotting the Figure 6.18, we assumed the antenna separation distance in the long base is 2λ (12 cm) and the short base is (λ) 6cm, true DOA is 45 degrees, and a number of samples of a received signal is 16384. While taking the average of the estimation error, we have calculated it 50 times.

6.2.3 Sampling Rate Versus Estimating Error

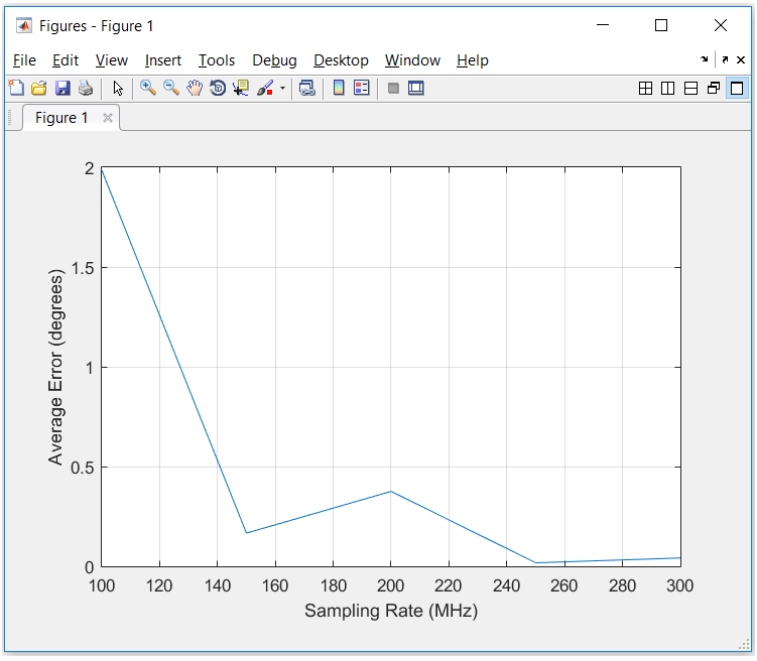

Figure 6.19: Sampling Rate Versus Average Estimation Error

Figure 6.19 shows that the minimum error occurs when we choose sampling rate as 250 MHz. Sampling Rate-vs-Average Error behaviour is inversely proportional. However, local increases cannot be explained in this study. According to knowledge extracted from simulation, the best choice for sampling rate is 250 MHz.

Same assumptions have been made while plotting the Figure 6.18, the antenna separation distance in the long base is 2λ (12 cm), and the short base is (λ) 6cm, true DOA is 45 degrees, and a number of samples of a received signal is 16384. While taking the average of the estimation error, we have calculated it 50 times.

7 Recommended System Parameters and Conclusion

According to the literature review and parameters provided by the project team, the modelling of the concept of the automatic antenna tracker has been done. As a result of computer simulations, we have done we reach some results for design parameters of the Automatic Antenna Tracker for Sounding Rockets.

7.1 Antenna Array Dimensions

The antenna array for the system has been designed with Sensor Array Design Tool of the MATLAB simulation software.

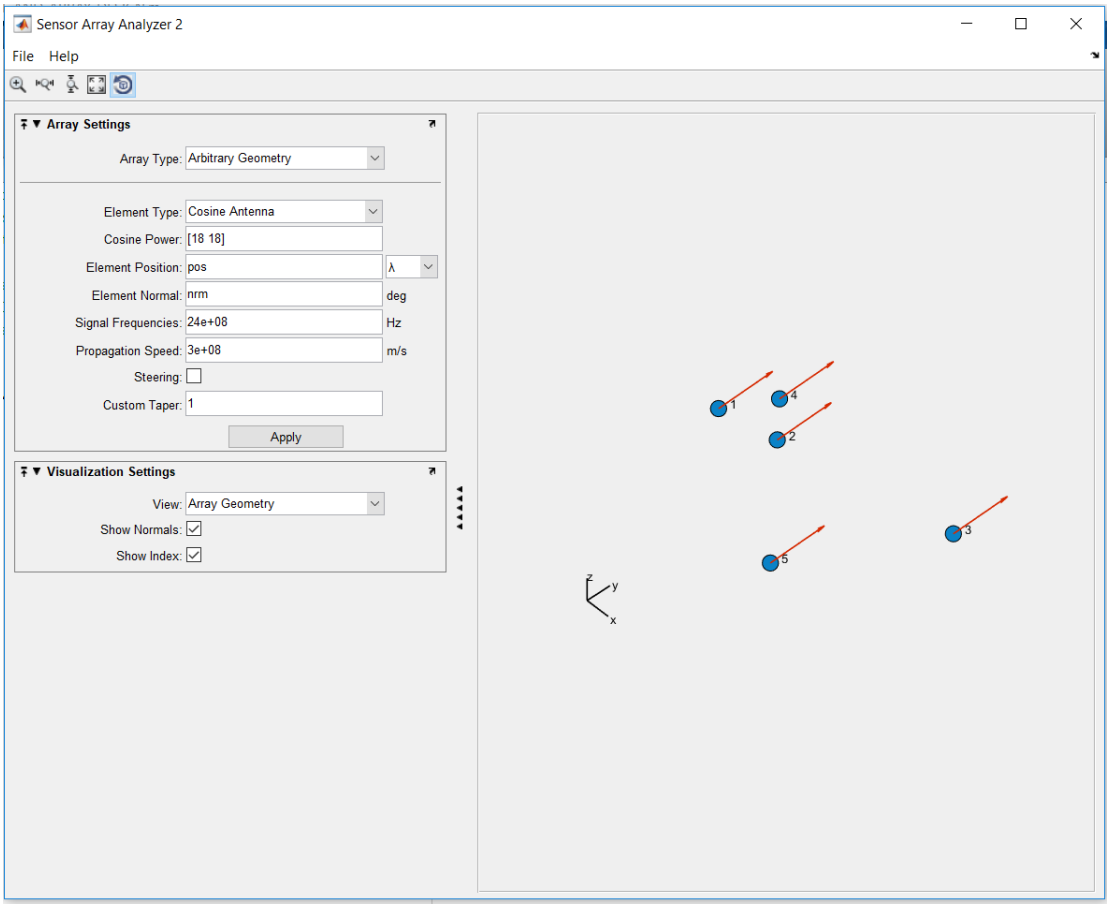

Figure 7.1: Sensor Array Analyser Screen and Antenna Array

The position vector is designed according to wavelength. As it is shown in Figure 6.16 the best performance is taken when the antenna separating distance between antenna 1 and antenna 3 (Long base for elevation dimension) equals to 2λ (12 cm) and the antenna separating distance between antenna 1 and antenna 2 (Short base for elevation dimension) equals to λ (6 cm). Therefore, distances between antennas recommended choosing in that way for azimuth and elevation sub-arrays.

7.2 Sampling Rate

The sampling rate depends on the Intermediate Frequency which the receiver reduces the 2.4GHz ISM band to. Sampling rate should be at least in Nyquist frequency. In the case of increase sampling frequency, the amount of the data should be processed increase. One of the most important requirements for the system is computation time and heaviness. Therefore, the best case is choosing sampling rate only high enough to satisfy error angle requirement for tracking.

In practice, digital receivers are sampling the signal with a delay which called jitter. Jitter causes the time delay between different antenna channels and this affect the phase estimation. We could not simulate the effect of the jitter for our system. However, according to the literature when the jitter is below than ten ps, the estimation error will not be catastrophic for tracking the sounding rocket [28]. For that reason, this should be considered while choosing ADC for a digital receiver.

According to Figure 6.18, the optimum case is choosing 250 MHz as a sampling rate.

7.3 Window Function

The key performance parameter for the window function is the gap availability in phase spectra for linear phase part. Cross-Correlation Interferometer is estimating the DOA according to the slope of the linear part of the phase diagram for the maximum bin of the frequency.

As it is analysed in the section 6.1.2.5, choosing the Gaussian window with $\alpha=3$ and window length $N=30$ is the best candidate for Antenna Tracking Direction Finder.

7.4 Analysis of The Average Taking Cross-Correlation Direction Finder

In the case of the digital processor or FPGA (Field Programmable Processor) is powerful enough to compute DOA fast for the sounding rocket, taking an average of the DOA results can also increase the performance of the system. Even though it seems random, Figure 7.2 shows that the performance can be increased by that way.

7.5 Future Work and Conclusions

The literature review shows cross-correlation Interferometer method also can be used in different spread spectrum telemetry signals [28, 29, 30].

This dissertation only analysed the case for single sounding rocket tracking. Multiple missile tracking or multiple satellite tracking would be good expansion for this study. To make this possible analysis of the Subspace DOA systems for automatic antenna tracking should be done as a future work. Even though the MUSIC method is computationally

heavy, the root MUSIC or ESPRIT method can be used. There are many studies about subspace methods in the literature.

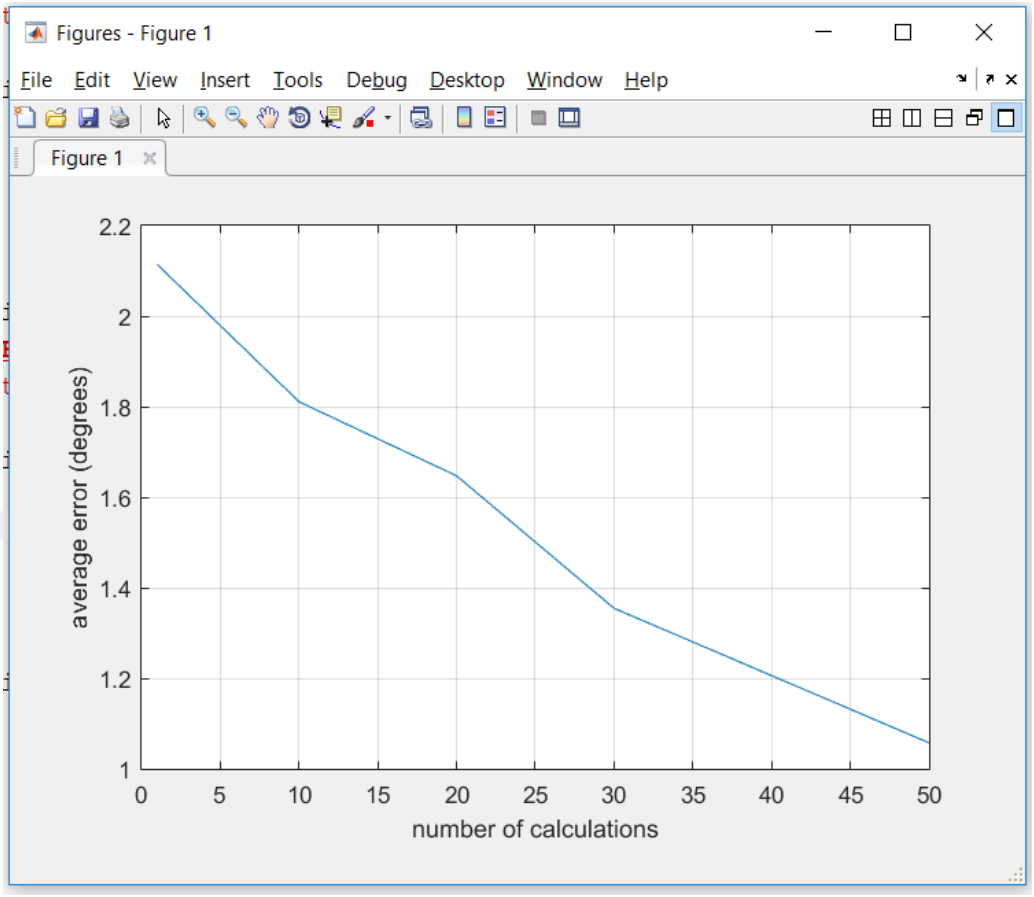

Figure 7.2: Number of Calculations-vs-Average Error

Implementation of the system is another work we could not do for the reason this is time constraint. Implementation can be done by a different student as a master study. In that work, the availability of the system recommended would be understood better. Another important work for Automatic antenna tracker is the controller and mechanical design of the tracker.

REFERENCES

[1] Sub Ik Lee, Kyung-WhanYeom, “A new technique to improve pointing performance for ship-borne mobile telemetry antenna system.” Advances in Space Research,2015.

[2] G. Chen, D. Grace, T.C. Tozer, “Evaluation of the effects of user antenna pointing error in multiple high-altitude platform systems” IET Communication Vol. 1, No.3, June 2007.

[3] Sultan Aljahdali, “Enhancing the Capacity of Stratospheric Cellular Networks Using Adaptive Array Techniques”,I. J. Computer Network and Information Security, 2013

[4] Tiago Varum, Joao N. Matos, and Pedro Pinho, “Detect and Pointing Algorithm’s Performance for a Planar Smart AntennaArray: A Review”, ACES JOURNAL, Vol. 30, August 2015.

[5] Bassem R. Mahafza,“Radar Systems Analysis and Design Using MATLAB, Chapter 11” Chapmen & Hall/CRC, 2000.

[6] Daniel Guerkin, Shane Jackson, Jonatan Kelly, “Passive Direction Finding: A Phase Interferometry Direction Finding System for an Airborne Platform”, Worcester Polytechnic Institute, October 10 2012.

[7] Eric Silva, Samantha O`Connor, Cristopher Massa, “The Beacon Locator Project: A Passive Direction Finding System for Locating Pulsed Emitter Signals”Worcester Polytechnic Institute,October 13 2011.

[8] Jeffrey Foutz, Andreas Spanias, Mahesh K. Banavar“Narrowband Direction of Arrival Estimation for Antenna Arrays”, Morgan & Claypool,2008.

[9] E. Jeff Holder,“Angle-of-Arrival Estimation Using Radar Interferometry Methods and Applications”, SciTech Publishing, 2014.

[10] Gawronski, W., Creparo, E.M., “Antenna scanning techniques for estimation of spacecraft position.”, IEEE Antennas Propag. Mag. 44 (6), 38–45. 2002.

[11] A. Kamerman, “Spread Spectrum Techniques Drive WLAN Performance.”, Microwaves & RF September, 1996, pp. 109-114

[12] Balanis, C.A., “Antenna Theory - Analysis and Design 2nded”, John Willey & Sons Inc., USA (1997)

[13] Balanis, C. A., Panayiotis I. Ionnides, “Introduction to Smart Antennas”, Morgan&Claypool, USA (2007).

[14] Balanis, C.A., “Modern Antenna Handbook”, John Willey & Sons Inc., USA (2008)

[15] Afacan, E., Aksoy, E., “Pattern Nulling in Linear Arrays with Fewer Elements by Using Differential Evolution Algorithm”, Eleco, Bursa, 260265, (2007).

[16] Elma, İ., “Anten Dizilerini Kullanarak Sinyal Kaynakları Tespiti”, Master of Science Thesis, The University of Zonguldak Karaelmas Institute of Natural Sciences, Zonguldak, Turkey, 2007.

[17] Roy, R., Kailath, T., “ESPRIT – Estimation of Signal Parameters via Rotational Invariance.

[18] Adcock, F., “Improvement in Means for Determining the Direction of a Distant Source of Electromagnetic Radiation”, British Patent 1304901919, 1917.

[19] Baghdady, E. J., “New developments in direction-of-arrival measurement based on Adcock antenna clusters”, Aerospace and Electronics Conference, 1989. NAECON 1989., Proceedings of the IEEE 1989 National, pp. 1873–1879 vol.4, May 1989.

[20] Kebeli, Murat, “RADIO DIRECTION FINDING & SMART ANTENNAS”, Master of Science Thesis, Bogazici Univesity the Institute for Graduate Studies in Science and Engineering, Istanbul, Turkey 2015.

[21] Denisowski, Paul, “An Introduction to Radio Direction Finding Methodologies”, Rohde&Schwarz, Pioneers in the Field of Wireless Technology, Symposium 2015.

[22] Products, R., A Comparison Of The Watson-Watt And Pseudo-Doppler DF Techniques, 1998, http://www.rdfproducts.com/wn004_apl_01.pdf, July 2009.

[23] KØOV, J. M., RDF FAQ, 1995, http://members.aol.com/homingin/FAQ.html, May 2008.

[24] Cianos, N., “Low-cost, high-performance DF and intercept systems”, WESCON/’93. Conference Record, pp. 372–376, Sep 1993.

[25] Schmidt, R. O., “Multiple Emitter Location and Signal Parameter Estimation”, Proc. Of RADC Spectrum Estimation Workshop, Griffiss AFB, NY, 243-258, (1979).

[26] Schmidt, R. O., “Multiple Emitter Location and Signal Parameter Estimation”, IEEE Trans. on Antennas and Propagation, AP-34:3, 276-281, (1986).

[27] Karabıyık, G. N., “Kablosuz Algılayıcılarda MUSIC Algoritması ile DOA Kestirimi”, Master of Science Thesis, Istanbul Technical University Institute of Natural Sciences, Istanbul, (2007).

[28] Finne, Magnus, “Methods for Direction Finding of Direct Sequence Spread Spectrum Signals”, Digital ESM Systems, May 1996.

[29] Houghton, Andrew Warren, “Time Domain Filtered Cross Spectral Density detection and direction finding of spread spectrum signals, and implementation using acousto-optic correlation.” PhD Dissertation, University of Plymouth, January 1996

[30] A.W.Houghton, C.D. Reeve, “Detection of Spread Spectrum Signals using the Time Domain Filtered Cross Spectral Density.”

[31] E. Oran Brigham, “The Fast Fourier Transform and Its Applications”, Prentice-Hall International Editions, 1988, p127.

[32] Johan Falk, Peter Händel, Magnus Jansson “Direction Finding for Electronic Warfare Systems Using the Phase of the Cross Spectral Density” Radiovetenskap och Kommunikation (RVK), Stockholm, Sweden 2002.

[33] Turgay KAYA, Melih Cevdet İNCE, “Pencere Fonksiyonu Aileleri ve Uygulama Alanlar”, Erciyes Üniversitesi Fen Bilimleri Enstitüsü Dergisi 26 (3): 291-306 (2010).